# Lunenburg Industrial Foundry & Engineering Propeller Study

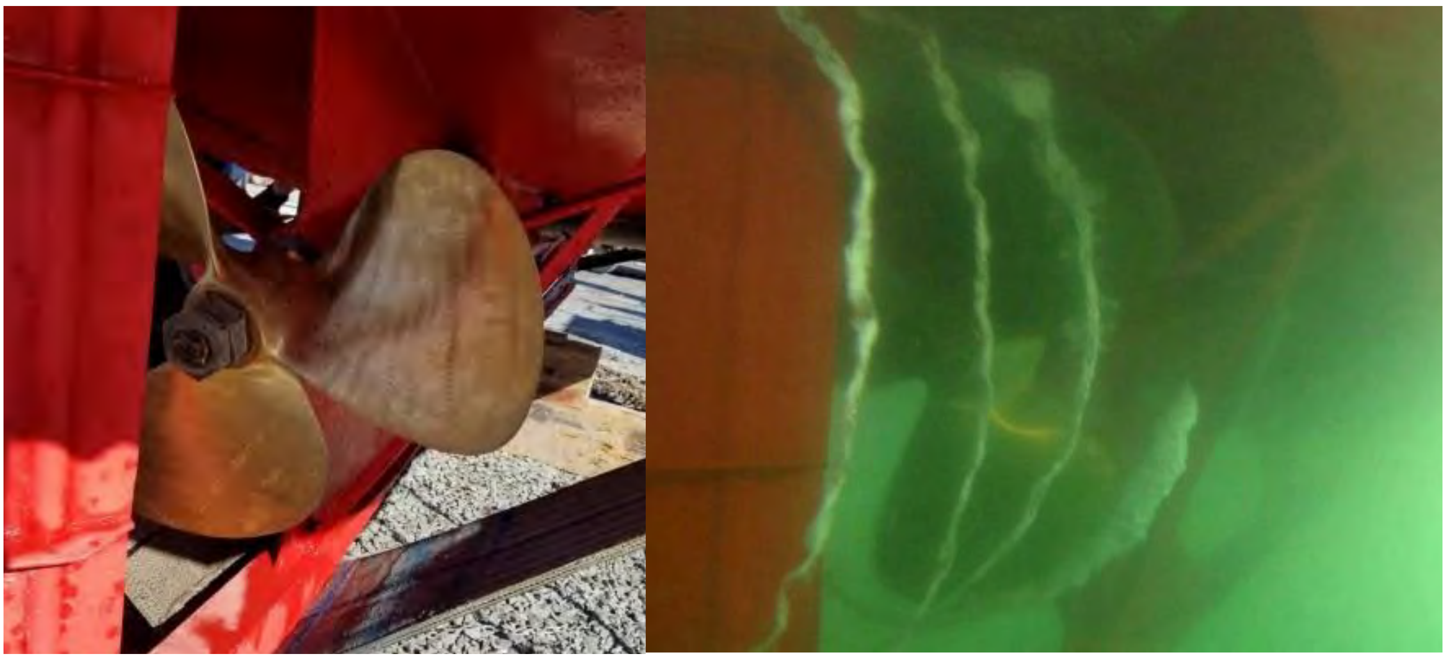

*Prepared by*

Nova Scotia Community College
Applied Geomatics Research Group
NSCC, Middleton, NS
Tel. 902 825 5475
email: tim.webster@nscc.ca

*Submitted to*

John Kinley
Managing Director
Lunenburg Foundry & Engineering Ltd.
53 Falkland St., Lunenburg, NS, B0J 2C0

How to cite this work and report:

NSCC Applied Geomatics Research Group. 2022. LUNENBURG INDUSTRIAL FOUNDRY & ENGINEERING PROPELLER STUDY. Technical report, Applied Geomatics Research Group, NSCC Middleton, NS.

Cover Figure: Left: The Acadian propeller installed on the LIFE Mascot. Right: A screen capture from GoPro video of Sea Trial 4, showing clear vortex cavitation starting with a mass of bubbles on the outer rim of the lower blade and showing three helixes that have been released from the propeller area. Image has been brightened by 20%.

# Table of Contents

## Table of Figures

## List of Tables

# 1 Introduction

In Canada's ocean playground, there is plenty of opportunity for the people of Nova Scotia to take to the waters, for both employment and recreation. Motorized seacraft often use a propeller to move the craft through the water, and it is critical that the propeller functions well and stays in good working condition. One of the most damaging impacts of water on the propeller blades is cavitation, which is basically when the pressures of the movements of the craft and the propeller blades interact with the pressure of the water itself to create a situation where the water along the blades will vapourize and form pits or cavities in the blade surface (Cult of Sea, n.d.). For the designers and manufacturers of propellers, being able to see evidence of cavitation while the propeller is in use is critical for general performance and consistency of the products as well as minimizing the impacts in future designs.

The researchers at the Applied Geomatics Research Group at NSCC (AGRG) were approached to lend their expertise to a study of the propellers designed and manufactured by Lunenburg Industrial Foundry & Engineering (LIFE) that would involve producing 3D models of the LIFE propellers and collecting data during sea trials to perform analyses of the propeller performance. The first stage of the project involved scanning and photographing three different propellers and using the resulting data to construct 3D models that were used for calculating metrics. Although LIFE has drawings and patterns of the propellers, they are fine-tuned manually during production, so AGRG captured high resolution "as built" laser scans and photogrammetric models of the propellers to possibly use in relating real-world performance characteristics back to the design and shape. The second stage of the project was to perform sea trials of the propellers, and for this phase AGRG researchers' experience with high precision positioning using Global Navigation Satellite System (GNSS) technology as well as with coastal processes (such as tidal currents and the effects of wind on currents) and underwater equipment were called on to be able to successfully capture data of a propeller in use during different conditions.

## 1.1 Study Area

The scans and photographs of the propellers were collected at the LIFE main office on Falkland Street, Lunenburg. The sea trials took place in Lunenburg Harbour, in lines running parallel to the marina (Figure 1).


**Figure 1. Study Area: The LIFE Foundry where scanning was done, and the area where sea trials were conducted in Lunenburg Harbour.**

# 2 Methods

## 2.1 3D Models

### 2.1.1 Data Collection

AGRG researchers travelled to the Lunenburg Industrial Foundry office to conduct laser scans and collect photos for the purpose of creating 3D models for three different designs of propellers: the Acadian, the Grand Banks, and the Bluenose. The propellers were hung on a small mount so that additional angles, such as the back of the propeller, could be captured with the laser scans and photos. AprilTag survey targets were placed around the propeller mount so that common points between laser scans of the same propeller could be more easily identified during the manual alignment process. As reflective surfaces do not scan well using photogrammetry, several steps needed to be taken to prepare the propeller's surface. First, a spray specialized for 3D scanning was used to impart a matte white finish on each propeller. Second, a black water-based paint was used to speckle the propeller to increase the level of surface detail that could be perceived by the photogrammetry software (Figure 2). Third, studio lights were placed around the propellers to minimize the number of shadows during the photo collection.

**Figure 2. A closeup of the hub of one of the propellers after it has been sprayed with the matte white formula and the black paint in preparation for being photographed and scanned.**

Two methods were used to create the propeller models, photogrammetry and laser scanning. For the photogrammetric models, a 16-megapixel Ricoh GR II camera was used to take photos sequentially in a circle around each propeller (Figure 3). High-resolution images of the propellers were essential for creating an accurate model. This step was repeated using different heights and angles to capture the propeller at multiple perspectives and ensure a maximum overlap between photos.

**Figure 3. The AGRG photographer (left) taking shots of the Bluenose propeller.**

In the second method, a Teledyne Optech Polaris terrestrial laser scanner was used to scan the propellers. The scanner was mounted on a Leica survey tripod with a tribrach fitting (Figure 4). The propellers were scanned from four positions around the propeller mounts to ensure quality scans of all angles of the propeller, and limit masking (shadowing) of one part of the propeller by another. Before each scan, the Polaris was levelled using the tribrach bubble level for coarse adjustments and the Polaris' internal electronic level for fine adjustments. Scan density was set to medium for all scans, resulting in a point spacing of approximately 0.5 mm. The vertical field of view for the Polaris was set at 120°. The horizontal field of view was set manually for each scan. The horizontal field of view was generally 30-45° and was kept as small as possible to reduce the time required for each scan.

**Figure 4. The Bluenose propeller being laser scanned (scanner on tripod to the right).**

### 2.1.2 Data Processing

The 3D laser scanning software, ATLAScan, was used to process the collected laser point clouds and remove noise from the scans. At the same time, Metashape photogrammetry software was used to create a dense point cloud of each of the propellers from the photographs that had been taken. Measurements of the propeller's hub diameter were taken in ATLAScan and used to create a local coordinate system in Metashape to accurately reflect the propeller's dimensions. Propeller measurements collected on-site were used to validate the metrics computed by ATLAScan. Comparing the processed data in each software program, photogrammetry produced a superior 3D model since it was difficult to filter out noise from the laser point clouds, resulting in distorted surfaces during subsequent surface reconstruction. The propeller mount also inhibited the laser scanner from fully capturing the back of the propellers, which largely contributed to the decision to use photogrammetric techniques for 3D model generation. A laser scan of each propeller model is displayed in Figure 5 with erroneous lidar points visible around the edges of the propeller blades. As the Polaris laser scans could not be accurately aligned to create a 3D mesh, the propeller surface from the single scan looks warped as the point cloud is rotated from the original collection angle. Table 1 gives examples of direct comparisons between photographs taken of each propeller, and the laser point clouds and photogrammetric meshes generated from the data collected.

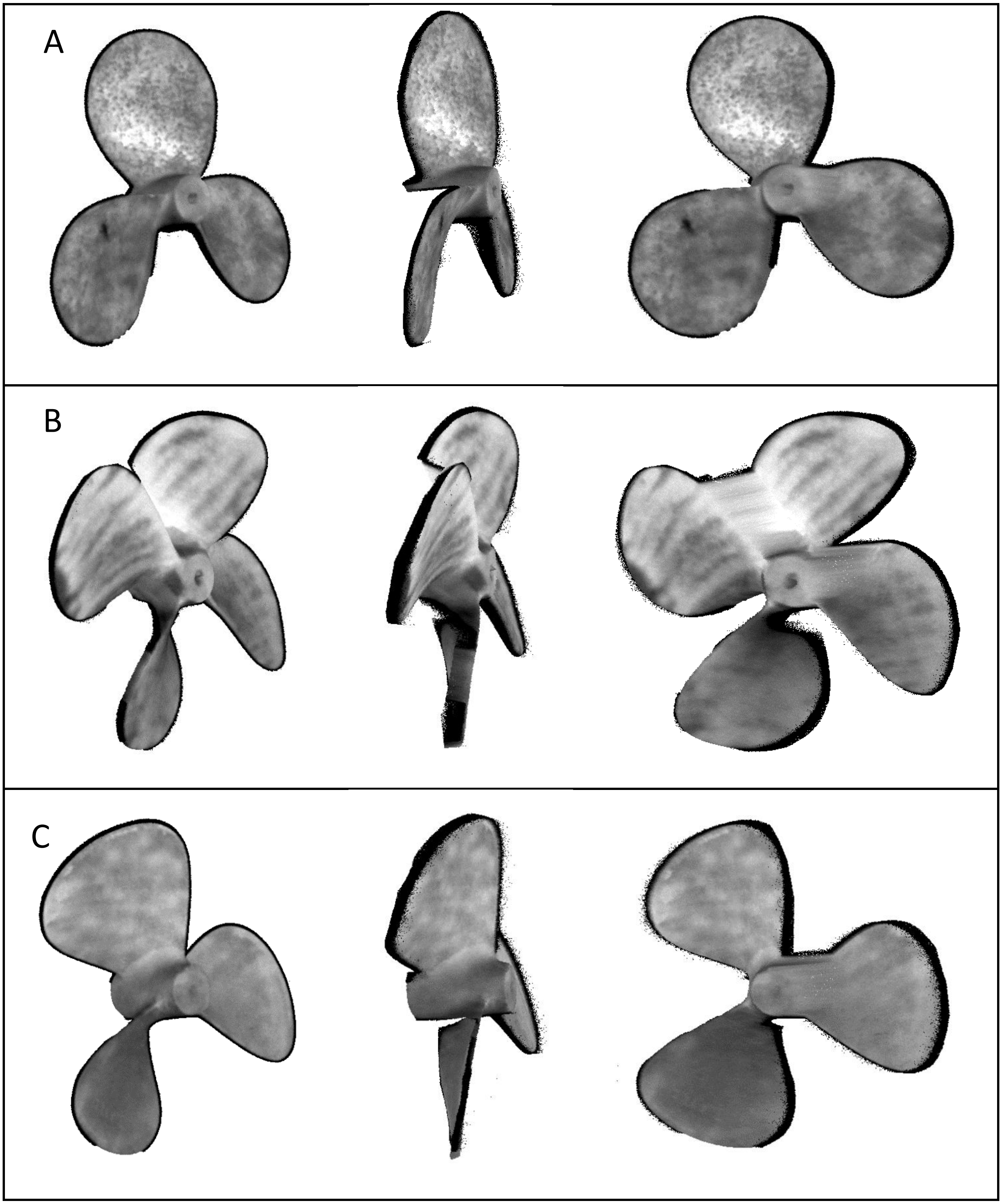


**Figure 5. A point cloud taken with the Polaris terrestrial laser scanner from a single scan of the Grand Banks (A), Bluenose (B), and Acadian (C) propeller models. The left-most images show the propeller at the orientation in which it was scanned.**

**Table 1. A table showing the results of the laser scanning and photogrammetric 3D modelling techniques matched with a photo taken by the Ricoh camera in a similar orientation and scale.**

| **Propeller Visualization Method** | **Propeller** | | |
|---|---|---|---|
| | **Grand Banks** | **Bluenose** | **Acadian** |
| Photograph |  |  |  |
| Laser Point Cloud | 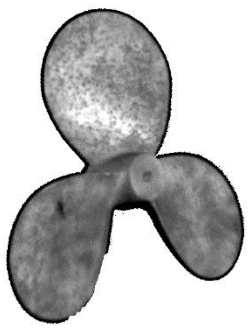 | 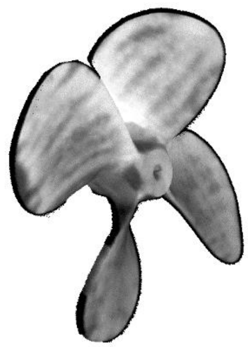 | 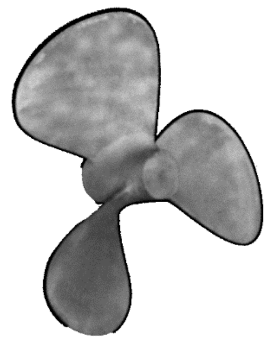 |
| Photogrammetric Mesh |  |  |  |

### 2.1.3 Blade Area Ratio Calculations

LIFE supplied documentation regarding the definition and calculation of different types of blade area ratios, primarily HydroComp Technical Report 135 "Blade Area Ratio Defined" (2007). HydroComp Inc. is an engineering company based in Durham, New Hampshire, USA that specializes in system design tools for naval architecture and propeller manufacture and design. Blade Area Ratio (BAR) is a parameter used to relate the size of the propeller back to its diameter and is used as a metric during propeller design as it is critical to controlling cavitation (HydroComp, 2007). There are three types of BAR – "projected", "developed", and "expanded". The "projected" area is the area of the outline as projected onto a surface below. “Developed” area is the area of the blade outline if it could be “untwisted”. “Expanded” area is what is found if the “developed” area could be flexibly unwrapped on a flat surface so that all sections were parallel (HydroComp, 2007). Once the collected imagery was processed and a coordinate system established, additional processing was performed in Autodesk Fusion 360 (detailed below) to enable the calculation of BAR for each propeller. The software used for this project did not support the calculation of the “expanded” area.

For each propeller, the virtual mesh image created in Metashape was imported into Autodesk, where the software tools were used to inspect each mesh for quality assurance. After they were approved, the software was used to virtually cut one blade off the propeller which allowed for the measurement of the area of the blade (Figure 6). As the BAR formula is based on the area of one side of the blade, the total blade surface area obtained above was divided by 2, and the result was then multiplied by the total number of blades on the propeller model being examined.

**Figure 6. A screen capture of a blade that has been virtually excised for measurement in Autodesk Fusion 360.**

The “developed” area ratio was calculated by dividing the total propeller area by the blade sweep path area (the area of the virtual circle drawn around the propeller when the blades are in motion). Having determined the total surface area of blades on each model in the step detailed above, the blade sweep path area was calculated by using basic geometry of circles, using $\pi r^2$ to compute the area of the propeller and subtracting the area of the propeller hub (Figure 7).

The “projected” area ratio was calculated using trigonometry, treating the blade like a right-angled triangle, using the manufactured pitch as the lower angle opposite the $90^o$ angle and using the measurements of the blade as the length of the side opposite the $90^o$ angle. Pitch and diameter metrics were provided by LIFE.

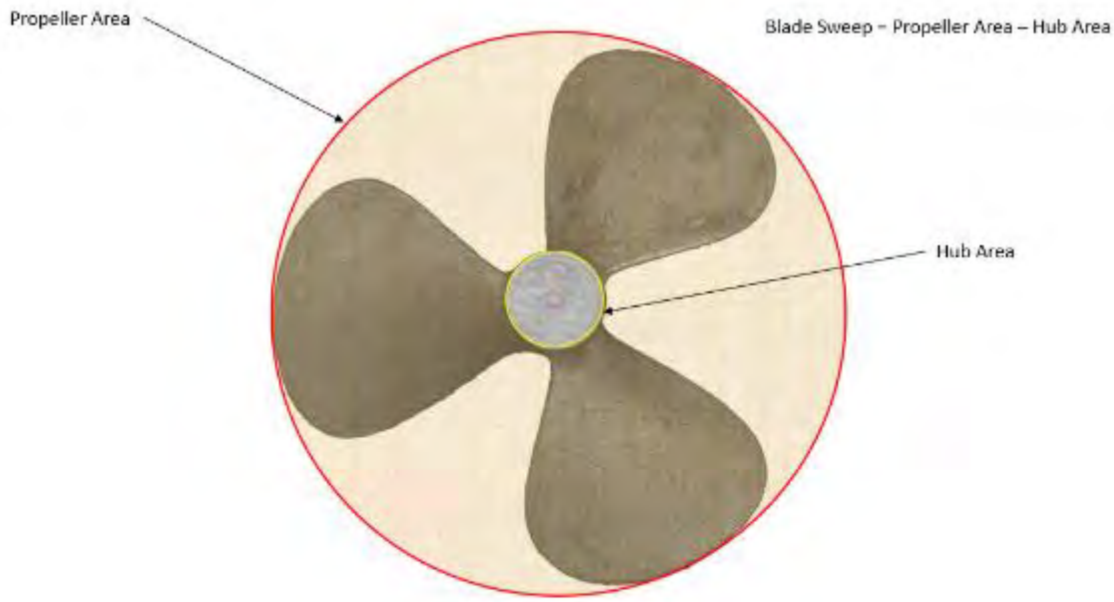


**Figure 7. A diagram showing how to calculate the blade sweep path area. The area of the total propeller area (red circle) is calculated, then the area of the propeller hub (yellow circle) is calculated. When you subtract the hub area from the total propeller area, the difference is the blade sweep path area.**

A verification of the AGRG calculated ratios was made by comparing them to the manually calculated ratio that is part of LIFE's standard procedures. LIFE uses the right side of the formula (HydroComp, 2007) shown below to manually calculate their ratio with their measurements and the known constants, so AGRG was able to use the PAR and DAR from this project in the left side of the formula to generate a ratio to directly compare to LIFE's results. The closer the AGRG ratios were to the LIFE ratios, the closer the 3D models would be to maintaining real-world properties and the more suitable they would be for use in analyses.

$$\frac{PAR}{DAR} = 1.067 - 0.229\,X\,\frac{P}{D}$$

where PAR = "projected area ratio" $P$ = pitch in degrees

DAR = "developed area ratio" $D$ = diameter of propeller in inches

A full list of the methods used to calculate "developed" area ratio and "projected" area ratio can be found in Appendix A.

## 2.2 Sea Trials

### 2.2.1 Data Collection

Sea trials were conducted by AGRG alongside staff from LIFE on February 24th, 2022, in Lunenburg Harbour. Although it was originally intended that each of the three propellers that had been modelled would also undergo sea trials, unforeseen delays meant only one propeller model, the Acadian, was mounted during the study (Figure 8). With the LIFE's Mascot hoisted out of the water, a mount custom designed by LIFE was installed next to the propeller and two GoPro underwater cameras were attached to it to capture the propeller behaviour (Figure 9, A1, A2, and A4). One camera was set to take pictures at a rate of 2 Hz while the other camera recorded video. A dive light illuminated the propeller while underwater (Figure 9, A3). AGRG installed a survey grade GNSS receiver to collect precise positioned reference points at a rate of 0.5 seconds to synchronize position and velocity with the timelapse data from the GoPro images and video. The collection of GNSS points was paused in between trials while the vessel was turned around to get back into position. Six trials in total were carried out with a track running parallel to shore, each with a successively faster velocity. The first, third, and fifth trial were run northwest, and the other three trials were run southeast. RPM and fuel consumption were not collected during the sea trials as LIFE's vessel did not have an accurate method to capture either metric. Each trial took between 1 – 4 minutes.

**Figure 8. The Acadian propeller design by LIFE installed on their Mascot on the morning of the sea trials.**


**Figure 9. The equipment to capture data during the sea trials: A) mounted on a (1) custom designed strut off the stern: (2) a GoPro to capture still images; (3): a dive light to illuminate the propeller; (4) a GoPro to capture video and B) GNSS equipment mounted on the boat to collect survey quality positional data.**

### 2.2.2 Sea Trial Conditions: Weather and Tide

Data from the Environment and Climate Change Canada weather station at Lunenburg was used to monitor environmental variables such as wind, temperature, and atmospheric pressure during the trials. The average wind speed and direction for the day have been charted in Figure 10, and they were approximately 40 km/h SE through the trial times. The predicted tide for Lunenburg was downloaded and used to understand the state of the tide during the trials and possible changes in current speed and direction (Figure 11). As is clear from the chart, the tide was rising during the duration of the sea trials.

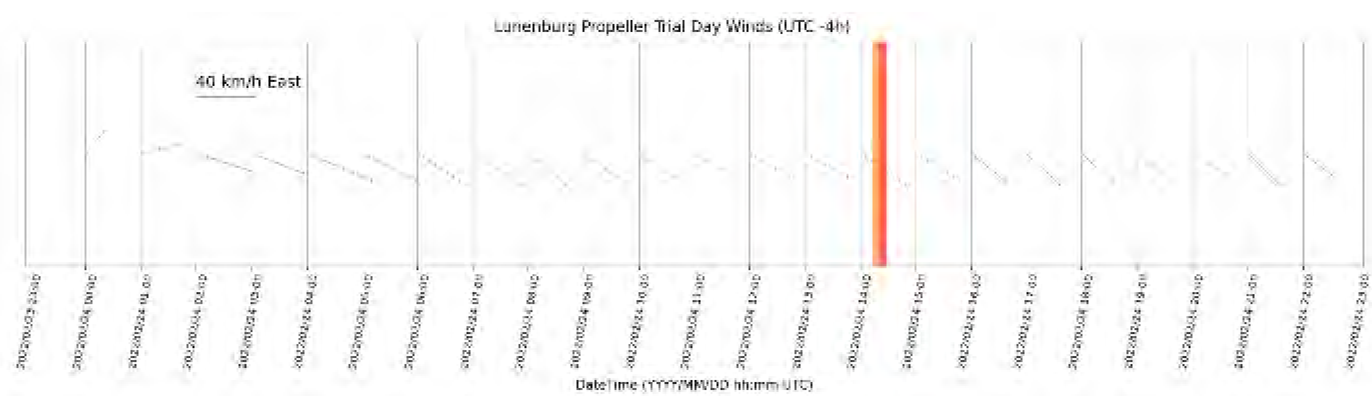


**Figure 10. A chart showing the average wind speed and directions for the day of the sea trials.**

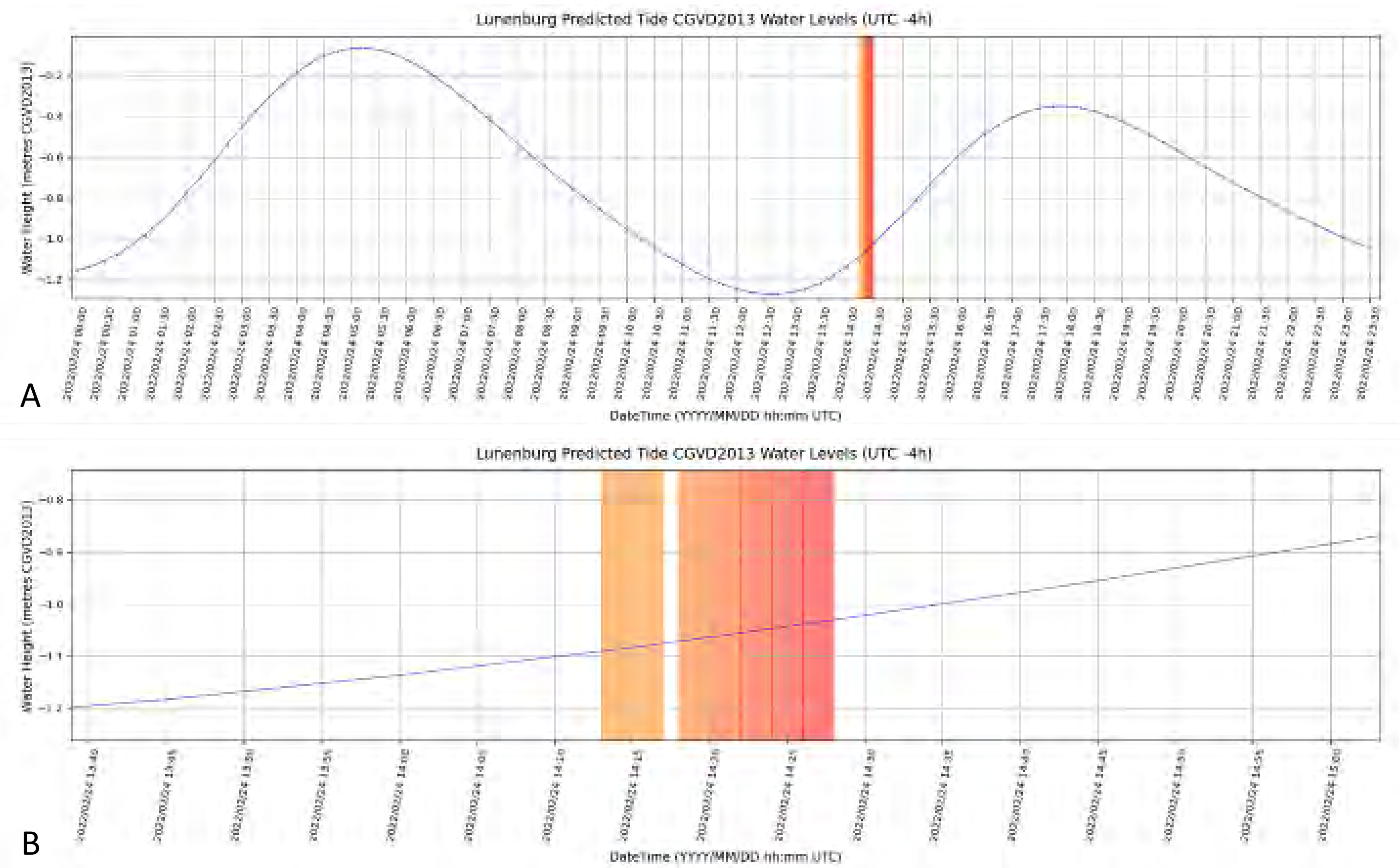


**Figure 11. Charts of the predicted tides for Lunenburg Harbour on the day of the sea trials. The shades of orange represent the different sea trials.**

### 2.2.3 Data Processing

AGRG downloaded the real-time kinematic (RTK) data collected by the GNSS equipment as a CSV file and converted it into an Excel spreadsheet, where it was processed to derive the geographic positions, velocity, and acceleration of the vessel at points along the sea trial runs. Velocity was derived by calculating the distance between locations of consecutive GNSS points and dividing those values by the amount of time elapsed between the points. The difference in velocity between consecutive points divided by the time elapsed was used to calculate acceleration. The timelapse information was exported along with the GoPro images. The time information was used to match the still images to the corresponding positional data, allowing the creation of a database linking the boat's movement to the associated images, and thence to the captured propeller behaviour. With both geomatic and time data matched, the data could be brought into GIS software such as ArcGIS Pro to be able to display the movements in a map with the added feature of being able to click on a discrete point to see the associated image of the propeller for that moment in the sea trial.

The video and still imagery were also examined manually to document evidence of propeller performance characteristics such as cavitation. Sheet cavitation would appear as a thin stationary sheet of bubbles or foam on the blade face (Figure 12A), and in some conditions this type can break down behind the blade as cloud cavitation; bubble cavitation is when distinctive bubble cavities are burned into the blade surface (this may not be detectable until the blade is examined out of the water); and vortex cavitation is when a helix or rope of water is formed either around the blade tips or at the hub of the propeller (12B) (Cult of Sea, n.d.). Timestamp information was again used to tie the captured images back to the movement of the vessel during the sea trials. It was determined that the GoPro still imagery was not always adequate as the frame rate was not capturing enough frames per second to see all the desired details, so AGRG saved frame by frame screen captures of key video segments for close, detailed analysis.

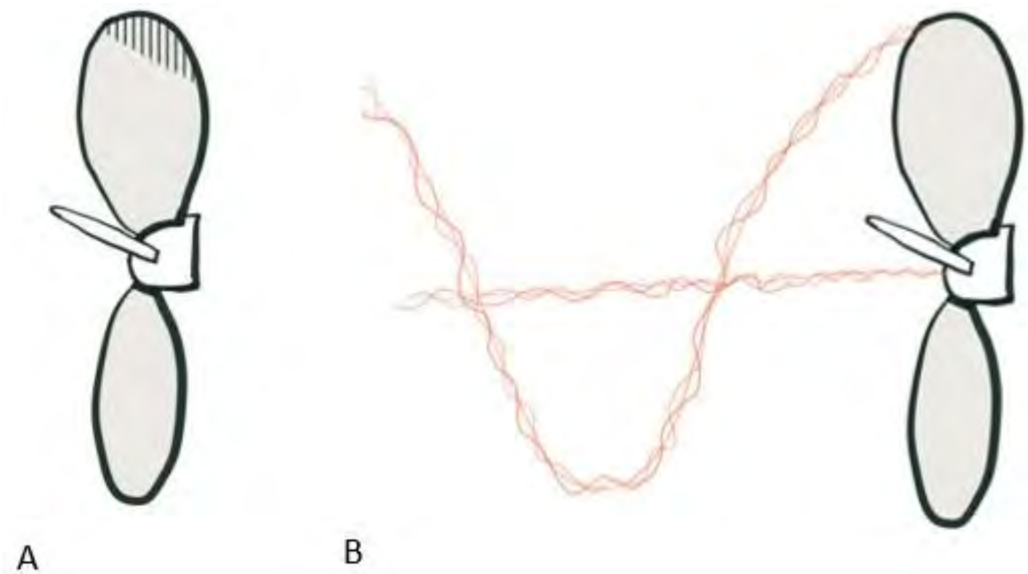


**Figure 12. A diagram showing sheet cavitation (A) and vortex cavitation (B) (Cult of Sea, n.d.).**

# 3 Results

## 3.1 3D Models

### 3.1.1 Images of 3D Models

The 3D models that were generated by AGRG show very fine detail, such as bumps, ridges, and notches visible on the propeller surfaces (Figure 13 to Figure 16). Flat images do not do the models full justice, as in the appropriate software they can be examined from all angles, flipped over, and manipulated to allow the viewer to see all parts of the propellers that were captured in the data collection process (Table 2). As seen in the data collection section of the methodology for the models, all efforts were made to make sure they hold true to real-world dimensions, so they can be used in calculations and analyses (2.1.3).

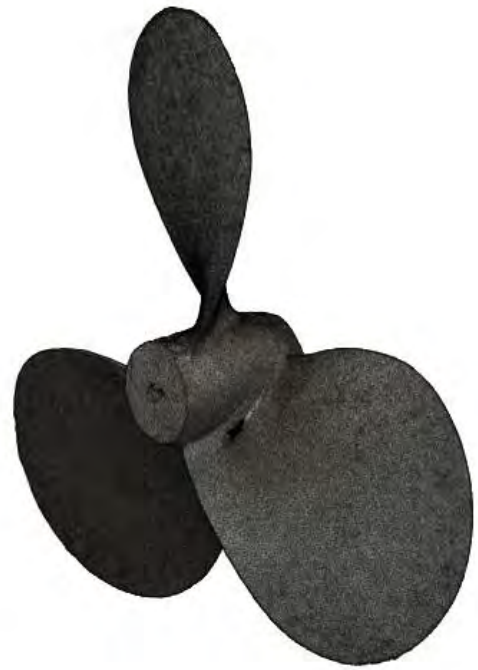

**Figure 13. The 3D model of LIFE's Grand Banks propeller, face on and ¾ view.**

**Figure 14. The 3D model of LIFE's Bluenose propeller, face on and ¾ view.**

**Figure 15. The 3D model of LIFE's Acadian propeller, face on and ¾ view.**

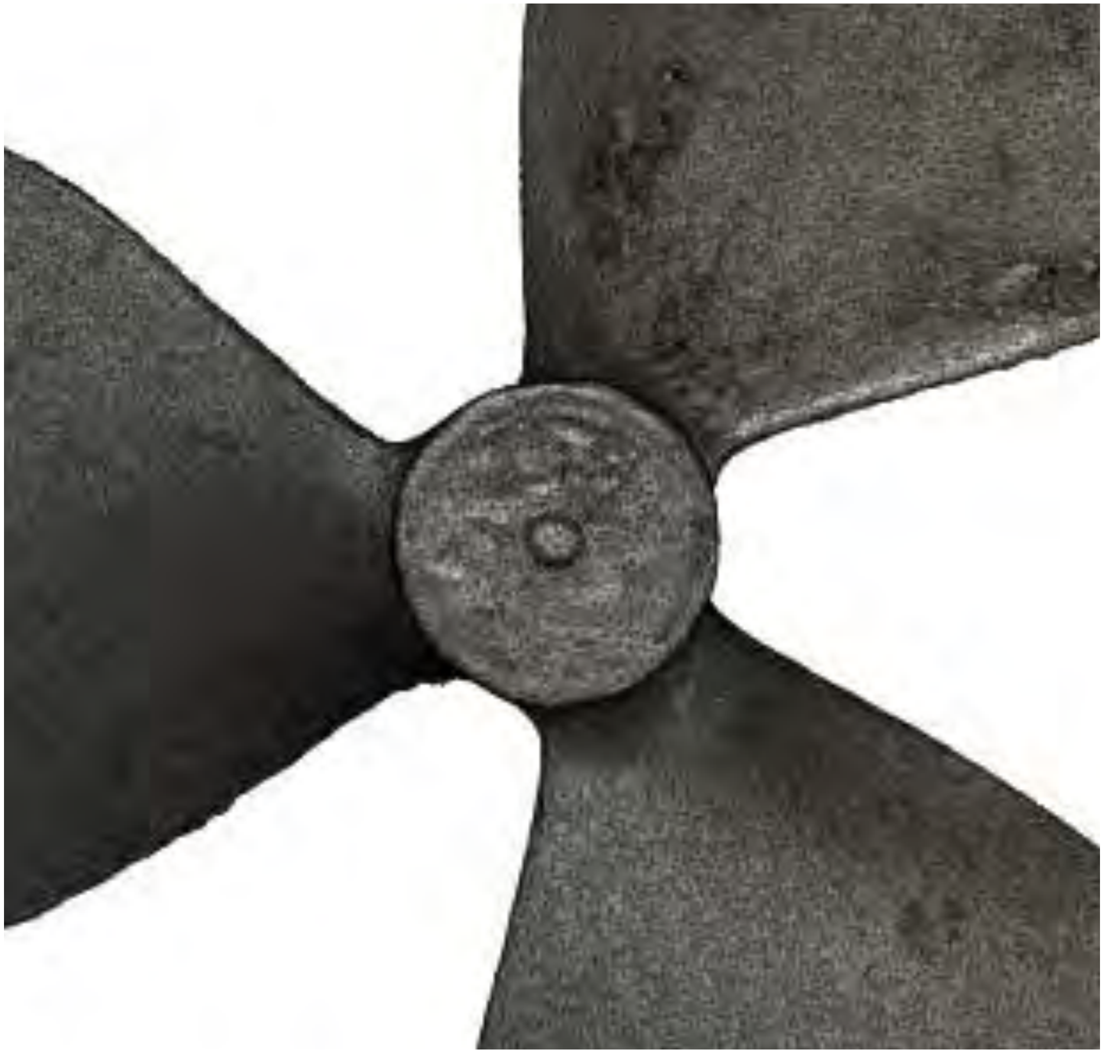

**Figure 16. A closer look at the details on the Acadian's hub.**

**Table 2. Different views of the 3D models of LIFE's propeller designs, showing the versatility of working with them.**

| **View of 3D Model** | **Propeller Model** | | |
|---|---|---|---|
| | **Grand Banks** | **Bluenose** | **Acadian** |
| Face On |  |  |  |
| Side View |  |  |  |

| **View of 3D Model** | **Propeller Model** | | |
|---|---|---|---|
| | **Grand Banks** | **Bluenose** | **Acadian** |
| Various Rotations |  |  |  |

#### 3.1.2 3D Models used in Blade Area Ratio Calculations

As outlined in the associated methodology section (2.1.3), the blade area ratio for the 3D model of each propeller was calculated and verified by being compared to the manually calculated ratio produced during LIFE's standard procedure, to test the reliability of the 3D models with real-world metrics. The results are summarized in Table 3; more details can be found in Appendix A.

**Table 3. Summary of Blade Area Ratio Calculations**

| Measurement/Metric | Propeller Design | | |
|---|---|---|---|
| | Grand Banks (3 blade) | Bluenose (4 blade) | Acadian (3 blade) |
| Area of one blade (front and back) | 1,938 $cm^2$ | 1,890 $cm^2$ | 1,903 $cm^2$ |
| Area of face of one blade | 969 $cm^2$ | 945 $cm^2$ | 951.5 $cm^2$ |
| Total blade area | 2,907 $cm^2$ | 3,780 $cm^2$ | 2,854.5 $cm^2$ |
| Calculated "Developed" Area Ratio | 0.57 | 0.74 | 0.56 |
| Calculated "Projected" Area Ratio | 0.53 | 0.63 | 0.47 |
| PAR/DAR (Calculated ratio) | 0.929 | 0.851 | 0.839 |
| LIFE's manually calculated ratio | 0.924 | 0.838 | 0.838 |

## 3.2 Sea Trials

#### 3.2.1 GNSS Position Tracking and Boat Metrics

The precise position points collected by the GNSS equipment mounted on the vessel were processed and imported into a GIS software to map the movement of the vessel in Lunenburg Harbour throughout the sea trials (Figure 17). Velocity and acceleration metrics were calculated for each of the sea trials and are displayed as graphs in Figure 18 to Figure 23. Average velocity between trials progressively increased with the first trial having an average velocity of 1.66 ± 0.27 m/s (3.23 ± 0.54 knots) and the sixth trial reaching a velocity of 4.16 ± 0.31 m/s (8.09 ± 0.60 knots). The difference in average velocity between the two final trials was only 0.06 m/s (0.12 knots), thus there was little difference in the amount of cavitation observed based on the GoPro imagery. As expected, acceleration values were highest during the first several seconds of the trials before reaching an equilibrium of no acceleration (0 $m/s^2$) when a constant velocity was achieved.

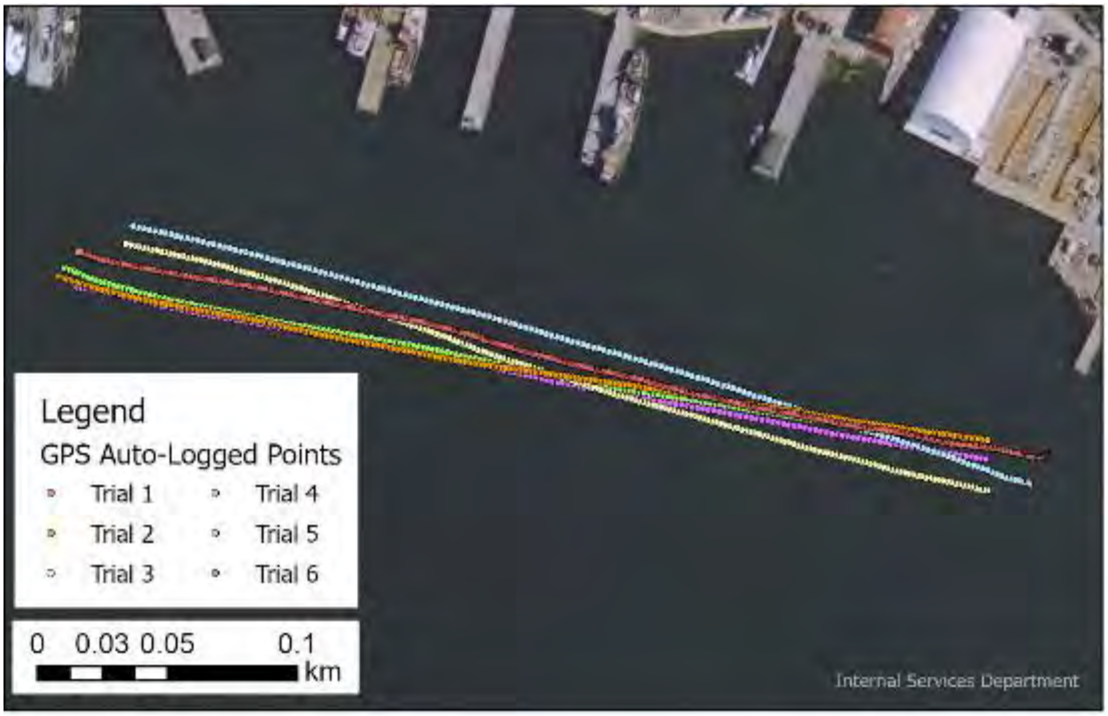


**Figure 17. A map showing the sea trials run in Lunenburg Harbour.**

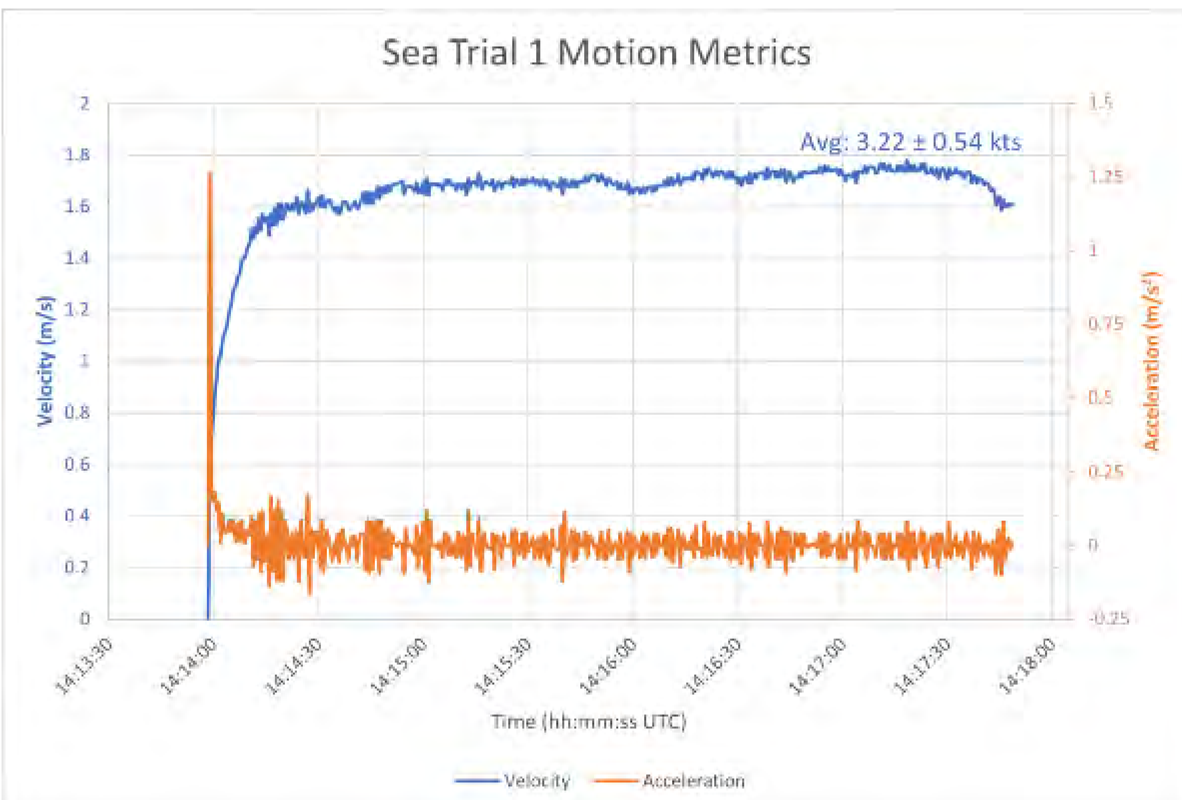


**Figure 18. A graph of the velocity and acceleration calculated during the duration of the first sea trial.**

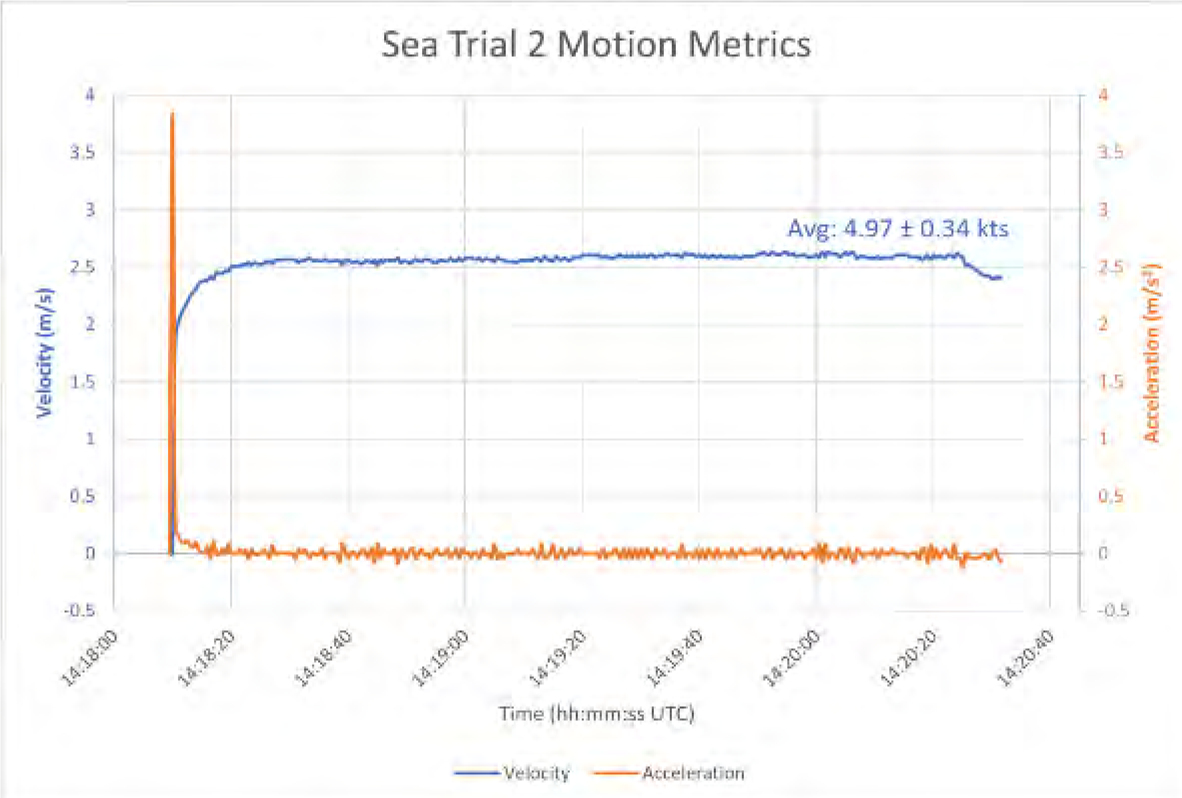


**Figure 19. A graph of the velocity and acceleration calculated during the duration of the second sea trial.**

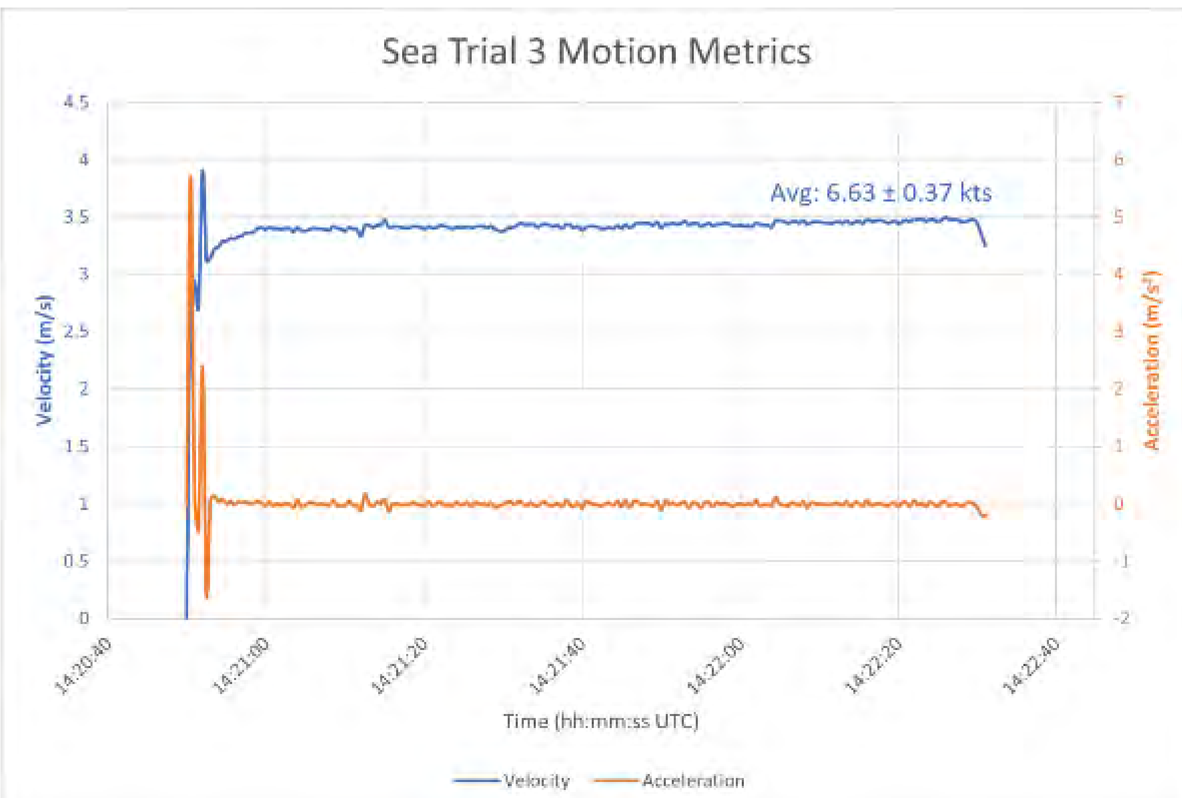


**Figure 20. A graph of the velocity and acceleration calculated during the duration of the third sea trial.**

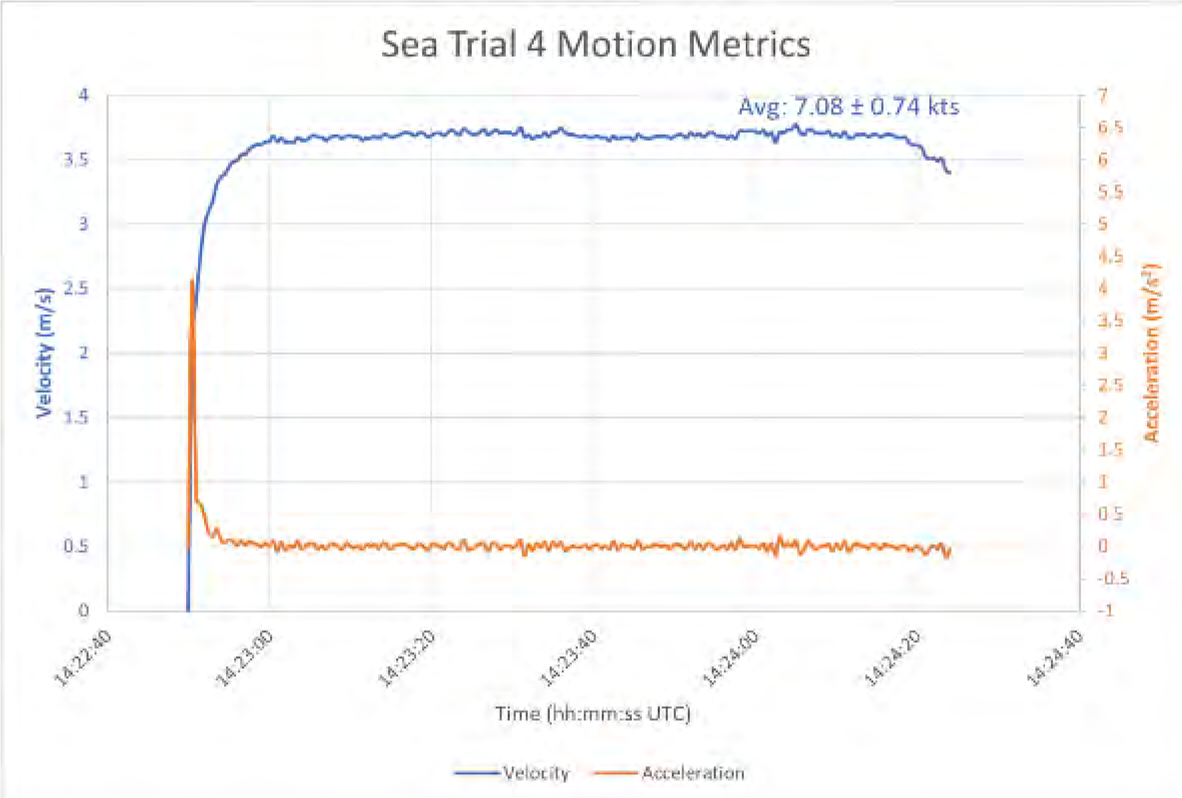


**Figure 21. A graph of the velocity and acceleration calculated during the duration of the fourth sea trial.**

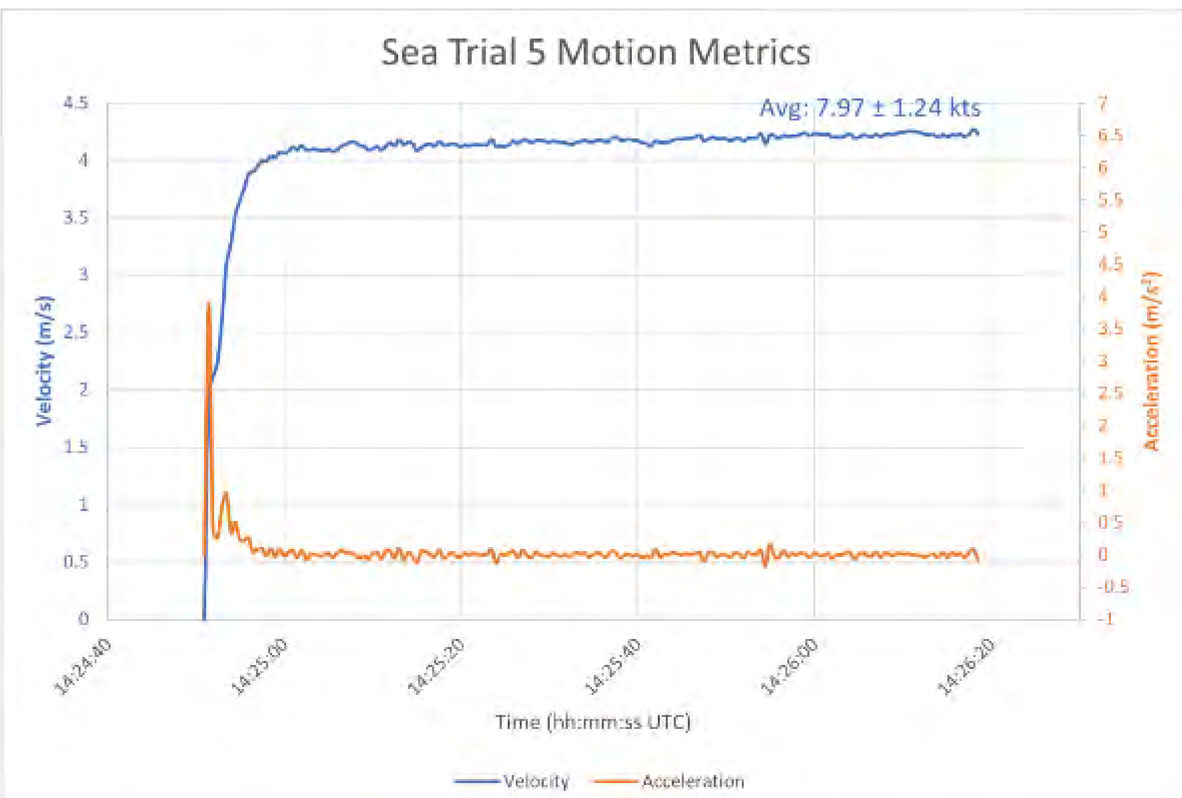


**Figure 22. A graph of the velocity and acceleration calculated during the duration of the fifth sea trial.**

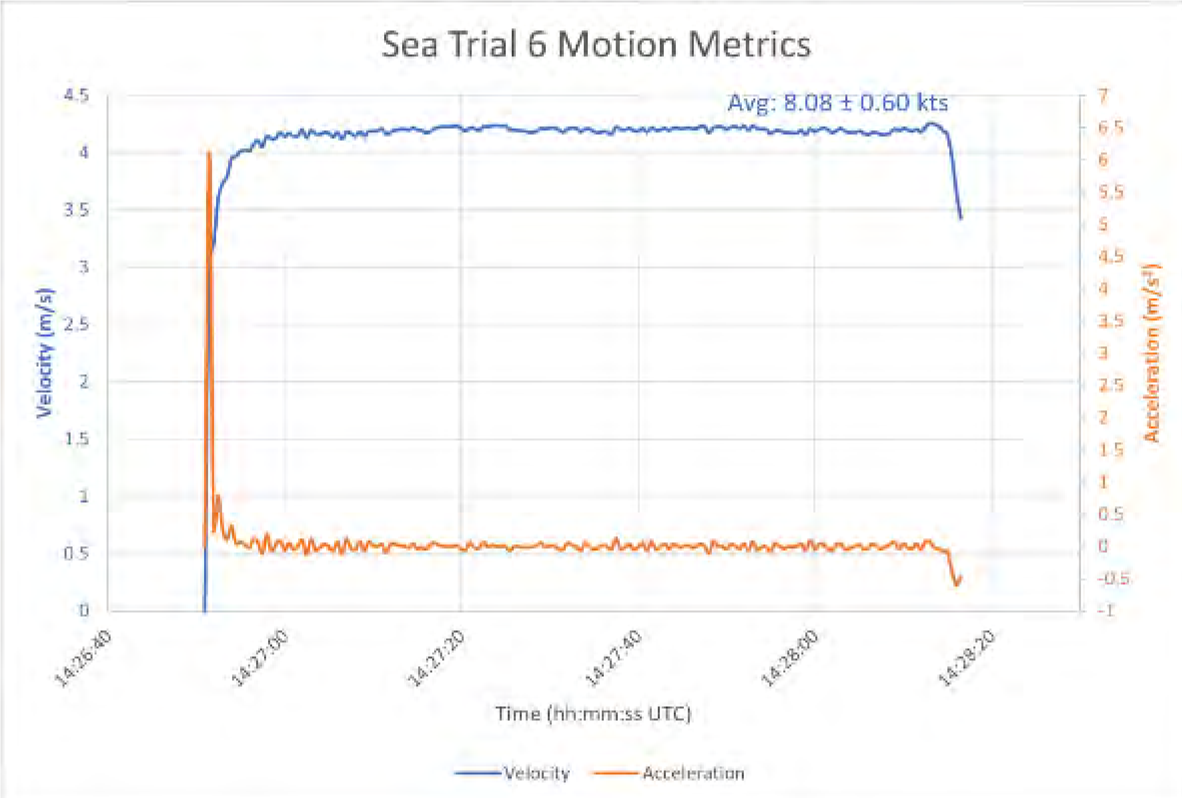


**Figure 23. A graph of the velocity and acceleration calculated during the duration of the sixth sea trial.**

### 3.2.2 Propeller Performance – Images and Video

It is important to preface this section with some notes on conditions that had significant impact on the imagery that was being reviewed. The water conditions were murky through much of the testing period, with haziness, debris, insufficient lighting, and water agitation between the camera and the propeller area interfering with the ability to positively identify incidents of interest; most of the underwater images in the report have had their brightness adjusted by +20%. There were also mechanical restraints that had an impact, such as camera speed not being fast enough to capture events or only capturing a small portion of an event, and most critically, the shifting of the GoPro cameras as the trials progressed. The still image camera shifted so that the propeller was no longer centered in the camera field of view and only the top half of the propeller was clearly visible. The GoPro camera taking video feed was completely dislodged from its mount during trial 4, with only the rudder strut remaining in view until the end of the test, meaning there was no video recorded during the two fastest trials of the day.

#### *3.2.2.1 Vortex Cavitation*

Many instances of cavitation occurred during the sea trials as observed through the collected imagery. The most identified type of cavitation seen was vortex, which can be identified by the rings of helices being released from the propeller blades and moving away from them or by a horizontal rope or vortex developing from the hub of the propeller. These clear visual indicators made vortex cavitation the most reliably identified occurrence.

By viewing video imagery frame by frame, it was possible to see how an incident of vortex cavitation began, as seen in Figure 24 below. In image A (top left) there is a cluster of bubbles to the left of the top right propeller blade which appears to be trailing off the edge of the blade; in image B the cluster has been drawn out, stretching between the top blades and starting to look more like a chain or rope of foam; and in images C through F the rope continues to follow around the arc of the blades sweep path, stretching thinner and staying tight to the sweep path near the rim of the blades, with a more diffuse foam cluster following it around. Once the rope flows around the blades to where it began, it tends to be released from the blades, moving as a ring of helix strands away from the blades and diffusing as it moves further from the propeller. In some of the documenting photos later in this section, it is possible to see multiple rings in one image.

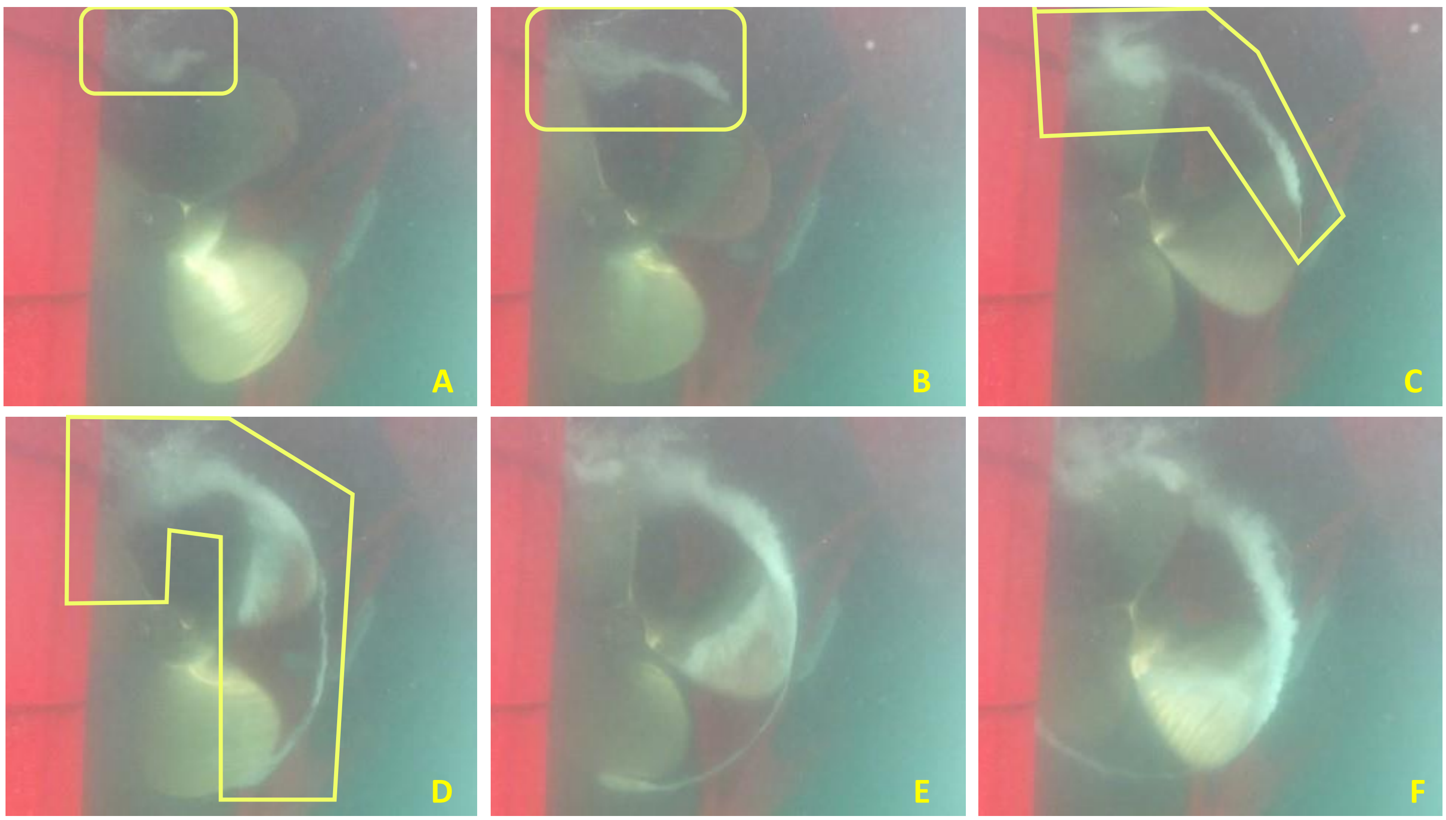


**Figure 24. The formation of a vortex cavitation spiral: A) bubbles forming a cluster between the top blades; B) the cluster is being stretched out into rope; C) the rope of bubbles is now following around blades and stretching along in an arc; and D – F) the bubble rope continues around the path of the blades, forming a ring around the propeller with foaminess still at top of blade area. (NB: images brightened by 20% from original)**

One aspect of cavitation that became clear as the images were examined is that it can impact both sides of the blades – the movement of the vortices generated by the blades is dependent on the direction the propeller is spinning. This can be seen below in Figure 25: in the left image, the propeller is in reverse and the vortices move towards the prow, whereas in the right the propeller is in forward and the vortices drift sternwards.

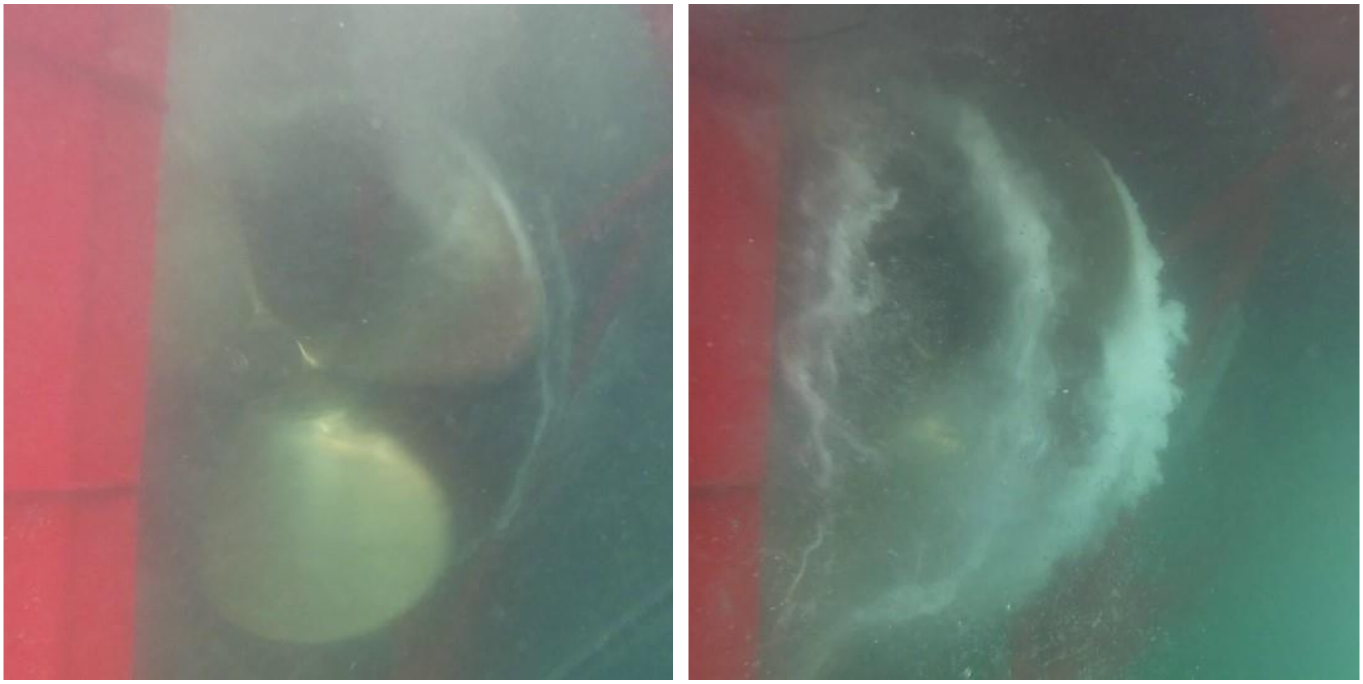

**Figure 25. The movement of the vortex cavitation is dependent on propeller direction: on the left the propeller is in reverse and the vortices are moving towards the prow, whereas on the right the propeller is in forward and the vortices move further away from the prow.**

Table 4 summarizes the observed instances of vortex cavitation, identifying which sea trial they occurred in and at what time, and the speed and acceleration of the vessel at the time. The images included in the first section of the table are screen captures from the associated videos, showing some of what was visible during the duration of the occurrence whereas those in the latter section are still images. This is not an exhaustive list, as there were times when it was difficult to determine if artifacts in the image were broken vortices or unrelated chains of bubbles from other sources. There is also another table detailing vortex cavitation instances in Appendix B; these instances were observed before and after the GNSS equipment was tracking the vessel, so no velocity or acceleration data is available for them.

It deserves to be noted that there is no definitive pattern to be found in when the vortex cavitation was observed during this project: it was seen at velocities as low as 0.79 m/s (1.54 kn) and as high as 4.23 m/s (8.22 kn) and was seen in times of both increasing and decreasing acceleration. Based only on the examples in Table 2, the highest frequency of clearly identified incidents happened during trials 1 and 4 (four incidents are listed for each of these runs) – but these runs were heading in different directions, with 1 being run with the wind at the back and run 4 being run into the wind.

**Table 4. Observed Instances of Vortex Cavitation**

| Image | Sea Trial | Time (UTC) | Velocity | Acceleration | Comment |
|---|---|---|---|---|---|
|  | 1 | 14:14:00 | 0.79 m/s<br>1.54 kn | 0.15 $m/s^2$<br>0.29 kn/s | Two vortex rings faintly visible to lower left under propeller blade, along with one free double helix floating towards the rudder. |
|  | 1 | 14:14:17 | 1.59 m/s<br>3.09 kn | 0.12 $m/s^2$<br>0.23 kn/s | Detached vortex strand on left side of image. Unable to determine if was generated by blades or was caused by an interaction of a burst of bubbles and the propeller. |
|  | 1 | 14:14:30 | 1.64 m/s<br>3.19 kn | 0.04 $m/s^2$<br>0.08 kn/s | Cloud of bubbles between top blades, could be beginning of vortex mass. |

| Image | Sea Trial | Time (UTC) | Velocity | Acceleration | Comment |
|---|---|---|---|---|---|
| 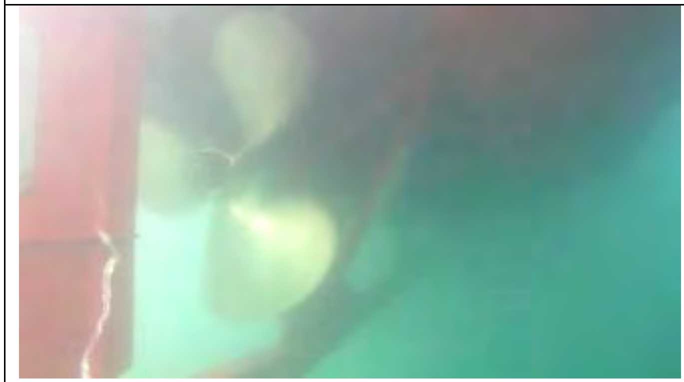 | 1 | 14:14:33 | 1.63 m/s<br>3.17 kn | 0.004 $m/s^2$<br>0.008 kn/s | A sudden helix strand passes by rudder – was only faintly visible in the propeller area in the previous screen. No other rings or foam trails visible. |
|  | 3 | 14:21:18 | 3.40 m/s<br>6.61 kn | -0.10 $m/s^2$<br>-0.19 kn/s | Faint but distinct vortex rings to right of propeller. |
| 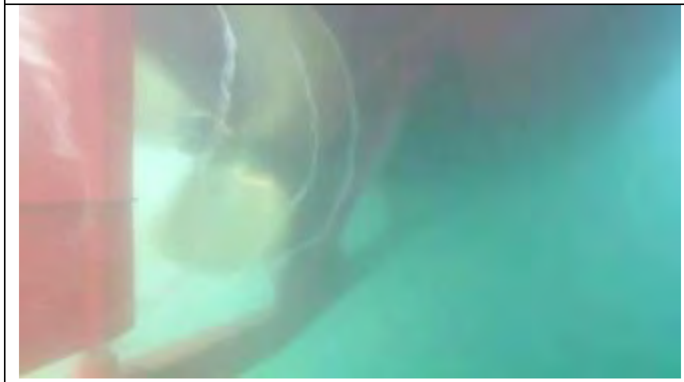 | 3 | 14:21:18 | 3.40 m/s<br>6.61 kn | -0.01 $m/s^2$<br>0.02 kn/s | Same time span, more intensity in vortex rings (more developed, closer together). |

| Image | Sea Trial | Time (UTC) | Velocity | Acceleration | Comment |
|---|---|---|---|---|---|
|  | 3 | 14:22:27 | 3.48 m/s<br>6.76 kn | 0.0008 $m/s^2$<br>0.002 kn/s | A horizontal helix strand is seen across the middle of the rudder; cannot tell if originated around the outer rim of the blades (no visible signs in that area in previous images of this timespan) or if came from hub of propeller, where there is a haziness. There had just been a blast of exhaust from the propeller shortly before this. |
|  | 4 | 14:23:11 | 3.65 m/s<br>7.10 kn | -0.05 $m/s^2$<br>-0.10 kn/s | Again, horizontal strands around the hub of the propeller shortly after an exhaust blast. |
| 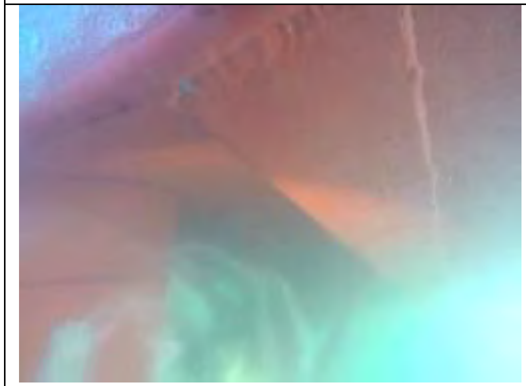 | 4 | 14:23:19 | 3.68 m/s<br>7.15 kn | -0.06 $m/s^2$<br>-0.12 kn/s | As well as the smoky vortex rings, there is a haze with some wispy lines around the hub.<br>*NB: this image appears different to the ones before and after it in this part of the table as it is a still image from the upper GoPro whereas the others are screen captures from the video from the lower GoPro.* |

| Image | Sea Trial | Time (UTC) | Velocity | Acceleration | Comment |
|---|---|---|---|---|---|
| 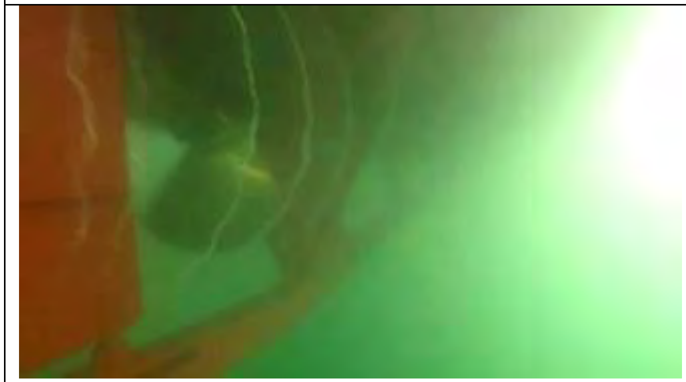 | 4 | 14:23:21 | 3.71 m/s<br>7.21 kn | 0.001 $m/s^2$<br>0.002 kn/s | Clear, tight vortex rings visible throughout this time period. |
| Note: after this point, all images are from the still image GoPro; the video images were no longer suitable as the camera was dislodged. | | | | | |
|  | 4 | 14:23:45 | 3.65 m/s<br>7.10 kn | -0.04 $m/s^2$<br>-0.08 kn/s | One unravelling helix faintly seen to right of propeller from about 1 o'clock down sweep path; center of hub area has many swirling lines in it, with a brighter area to right of hub (lighting or haze?) |
| 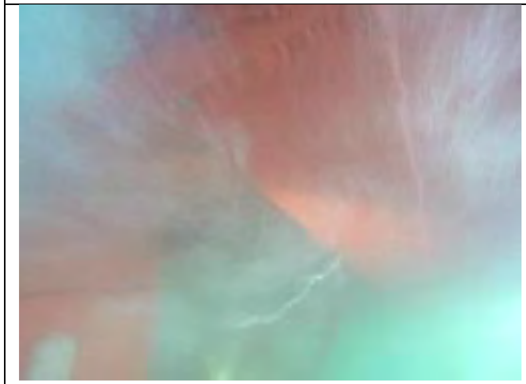 | | 14:24:29 | Note: caught between sea trials 4 and 5 so no GNSS data available | | Clear helix lines to right of midline of frame extending left and down. Can see twisting. Cannot determine source due to amount of foam and streaking off boat - line was just beginning to be visible in previous captured image to right side under boat, farther from propeller area |

| Image | Sea Trial | Time (UTC) | Velocity | Acceleration | Comment |
|---|---|---|---|---|---|
|  | 5 | 14:25:19 | 4.14 m/s<br>8.05 kn | -0.02 $m/s^2$<br>-0.04 kn/s | Two frames after rudder shift complete, have clear helix and haze: along top to tip of blade, down right side of blade edge sweeping towards bottom, with diffuse helix handing at rudder edge below centerline, left frame. Possible haze in front of hub and to right in blade area. |
| 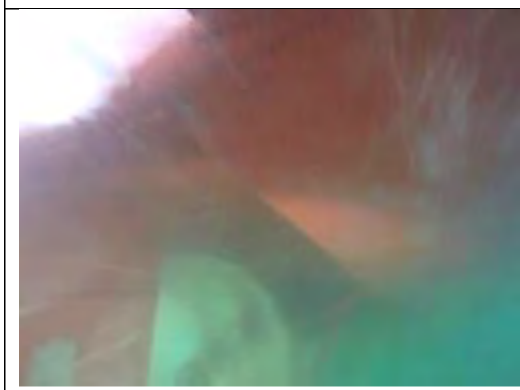 | 5 | 14:25:23 | 4.18 m/s<br>8.13 kn | 0.09 $m/s^2$<br>0.17 kn/s | Three double helix lines arcing along sweep path, from center of frame to left frame in front of rudder. Also, wispy twisting helix perpendicular to propeller, just below frame center on left in front of rudder. Wispy lines around hub and above it. |
| 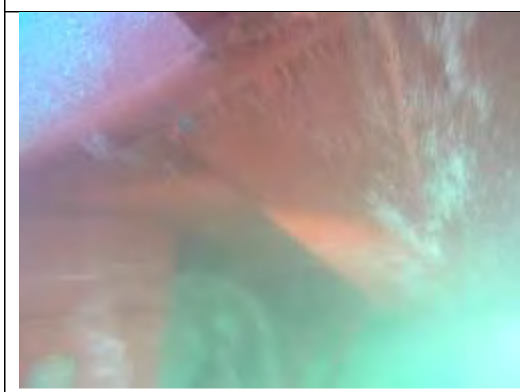 | 6 | 14:27:19 | 4.23 m/s<br>8.22 kn | 0.001 $m/s^2$<br>0.002 kn/s | After a rudder shift, see very distinct helix lines from propeller area, three following arc of sweep path of blades, two horizontal lines mid top rudder and very top along boat bottom. |

| Image | Sea Trial | Time (UTC) | Velocity | Acceleration | Comment |
|---|---|---|---|---|---|
| 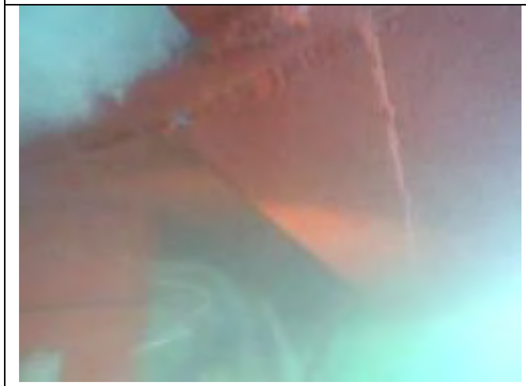 | 6 | 14:28:02 | 4.18 m/s<br>8.13 kn | -0.51 $m/s^2$<br>-0.99 kn/s | Vortices still being formed. Note wispy deformed S curve line beside rudder. |

#### *3.2.2.2 Sheet and Cloud Cavitation*

Sheet cavitation is when a thin layer of stationary foam or bubbles forms and clings onto the blade face, and cloud cavitation is when this mass of agitated water is released behind the blades. These forms of cavitation were much harder to successfully identify in the imagery from the sea trials, due to many factors outlined in the Discussion section of this report. Figure 26 does document a possible moment of both sheet and cloud cavitation, with the beard-like mass of foam around the edge and up the left side of the bottom blade and the mass of foamy or smoky white seen around the vortex rings behind the propeller.

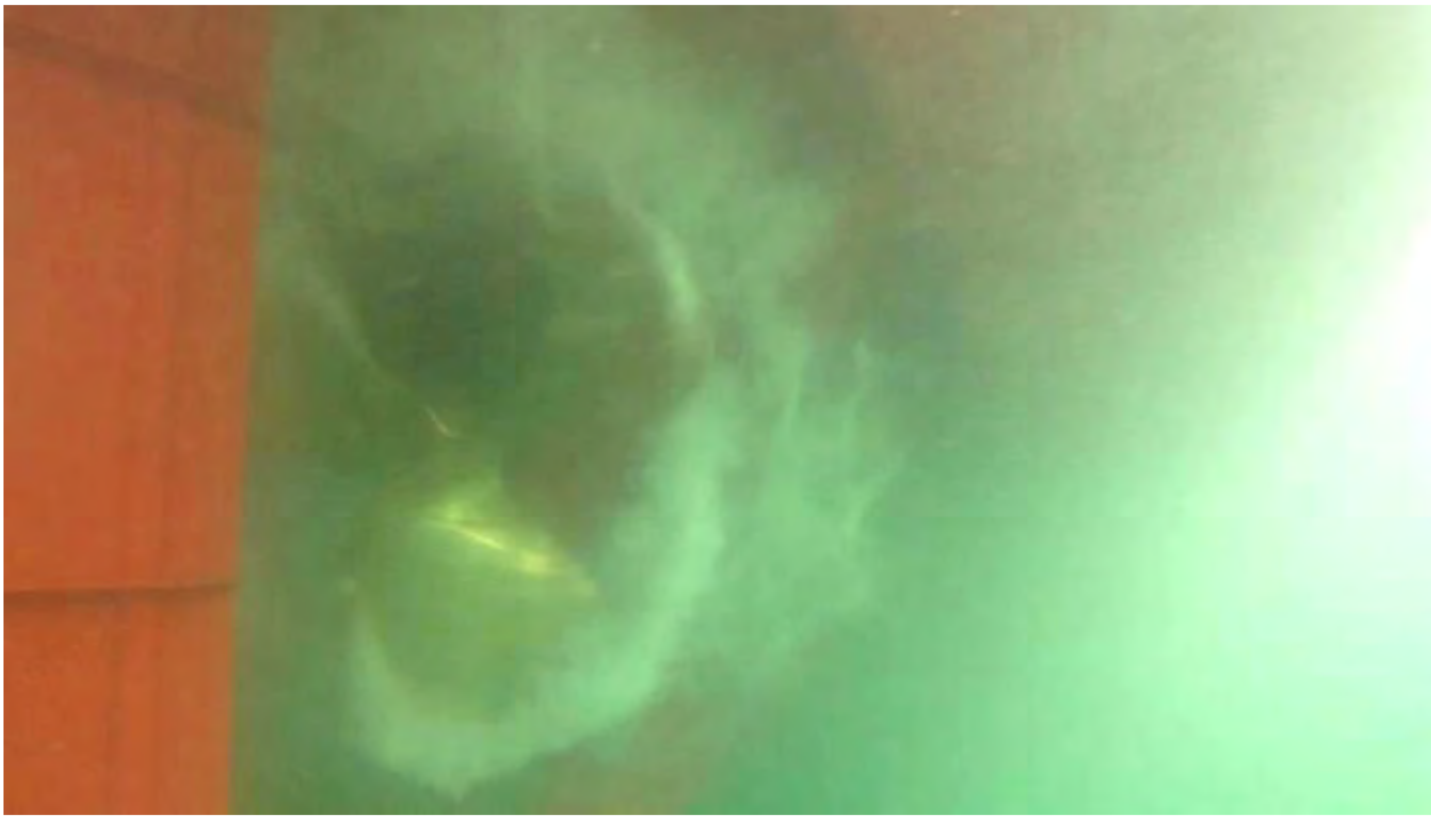

**Figure 26. A possible instance of sheet cavitation on the lower blade face; cloud cavitation may also be occurring behind the propeller.**

# 4 Discussion

## 4.1 3D Models

Photogrammetric techniques were used to create highly detailed and real-world scaled 3D models of three of LIFE's propellers: the Grand Banks, Bluenose, and Acadian. Two blade area ratio metrics, "developed" area ratio and "projected" area, were calculated for each propeller model. The accuracy of the BAR metrics obtained from the 3D models was assessed by comparing AGRG's calculated PAR/DAR ratio to the manually calculated ratio used by LIFE that is generated using propeller diameter and blade pitch with known constants. The difference in percentage between AGRG's PAR/DAR values and the manually calculated ratios from LIFE for the Grand Banks, Bluenose, and Acadian propellers were 0.54%, 0.02%, and 0.12%, respectively. Based on the minimal difference between the compared AGRG and LIFE generated ratios, it is evident that the 3D models provide an accurate visual and dimensional rendering of the photographed propellers. The 3D models will thus be a great resource for LIFE's quality assurance and design efforts to minimize the impact of cavitation on their propellers.

As is the nature of photogrammetry, the accuracy of the models was highly dependent on the quality of the images collected. Stage lights were used to improve the lighting conditions while photos were collected, however, there were several windows in the room which occasionally contributed to shadows in the imagery. Although best efforts were made to ensure the propellers were always in focus while collecting the images, a few blurry photos of the Acadian propeller may have resulted in an exaggeration of the dimpling of one of the propeller blades. (Figure 29A). The BAR calculation of the Acadian propeller may have been slightly affected by this. Additionally, there are some holes on the hub of the propellers that are likely the result of insufficient imagery captured over those regions of the propellers (Figure 30). These artifacts would not have impacted the BAR calculations for each of the propellers.

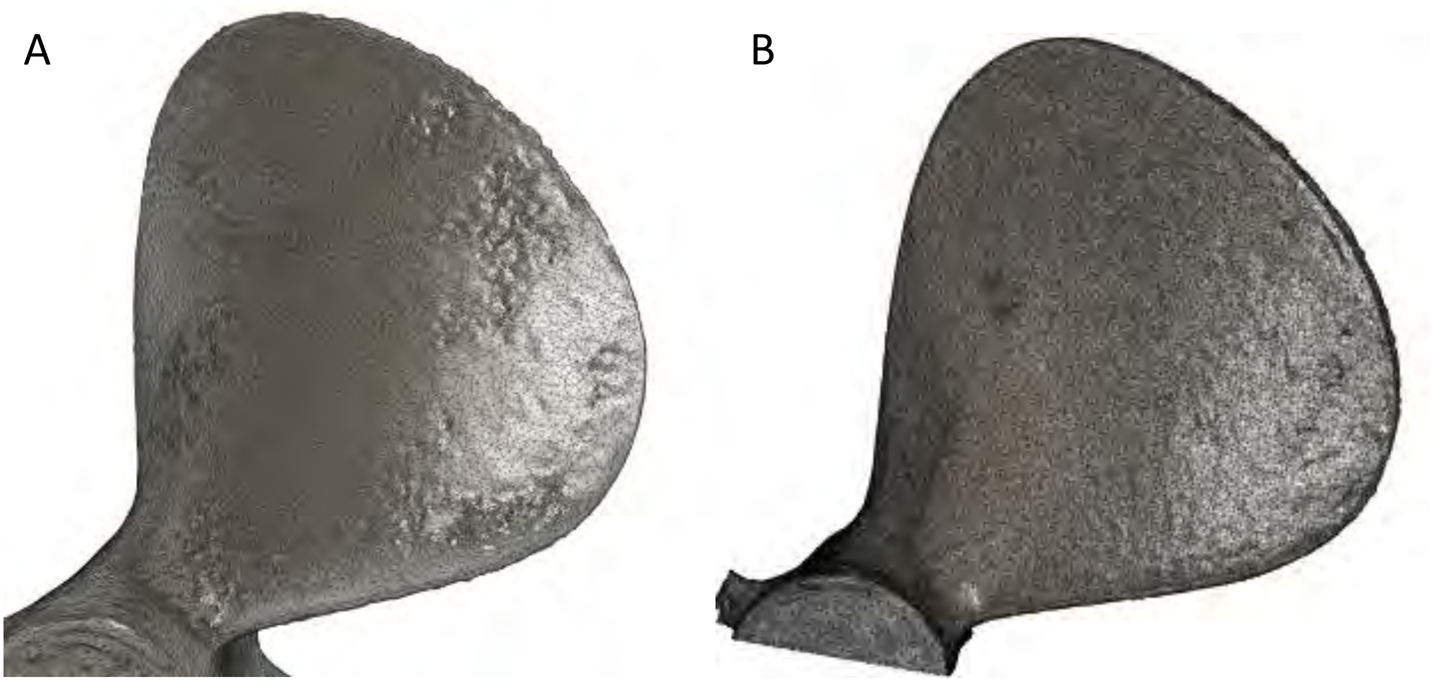


**Figure 27. Zoomed-in views of the back of the Acadian 3D model. A: The surface of one propeller blade shows a slight dimpling that may be erroneous. B: The surface of a different propeller blade is primarily smooth and shows little dimpling.**

**Figure 28. A side view of the Grand Banks 3D model. A small hole is visible on the hub of the propeller.**

## 4.2 Sea Trials

### 4.2.1 GNSS Tracking, Vessel Metrics, and Imagery

The GNSS equipment functioned well, and the data collected allowed for the calculation of vessel velocity and acceleration throughout the sea trials. As the collection of GNSS points was paused between trials as the vessel turned around, the initial acceleration determined between the first two consecutive points may be larger than the actual acceleration because the vessel was often already in motion as the trial began. Unfortunately, the RPM gauge on the LIFE Mascot was not functional, and so no metrics on this could be collected. As well, there was no way to determine fuel consumption during the trials, which would be of interest in studying the propeller performance.

There was an issue with the synchronization between the GoPro camera taking still images and the GNSS equipment; although the camera was set to match the GNSS capture rate of 2 Hz (which would be the equivalent of 2 pictures/second) it was discovered that the camera was taking images at a rate of 3 pictures/2 seconds, causing a sort of stuttering clustering of points when they were linked to the imagery (Figure 29).

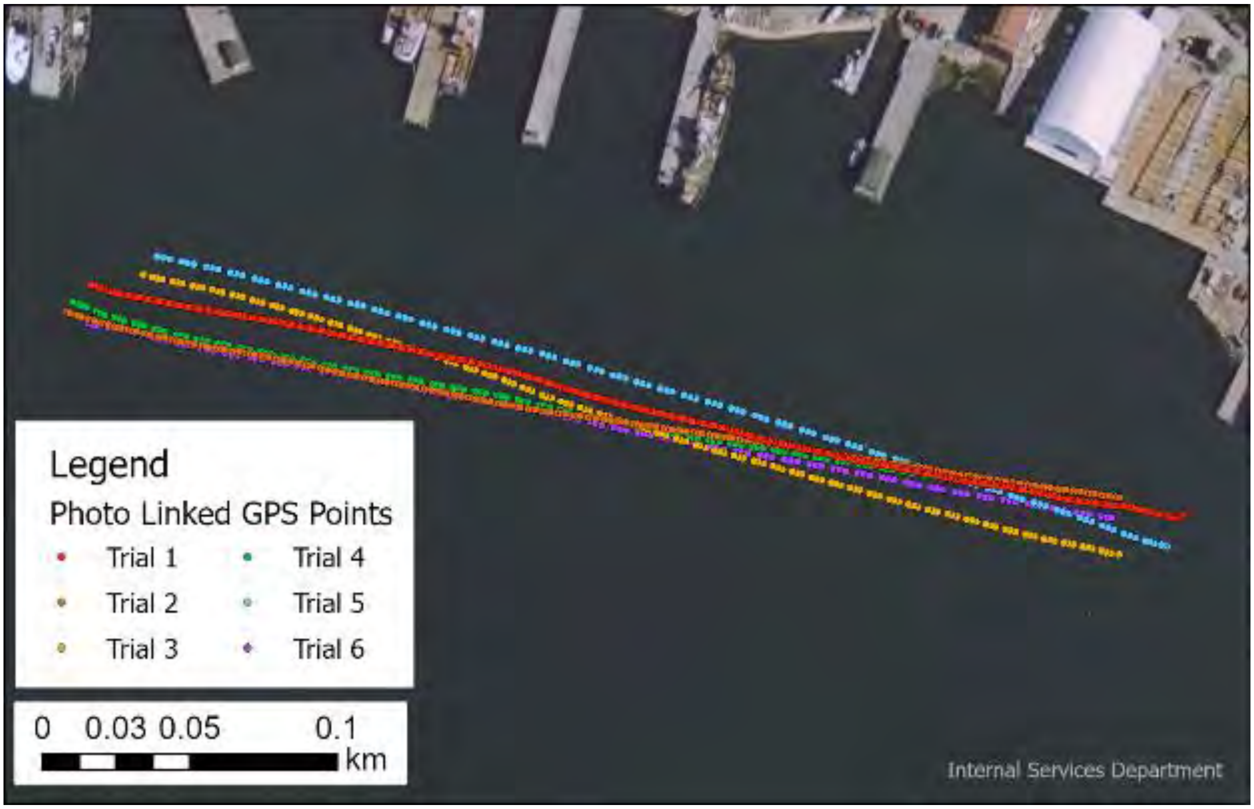


**Figure 29. A map showing the GPS points collected during the sea trials that were linked to GoPro images.**

### 4.2.2 Imagery Analysis for Cavitation

The most commonly identified type of cavitation seen during the sea trials was vortex, although this may be due as much to the camera view of the blades and the imagery quality as the actual frequency of occurrence of the other types – the images are often murky, especially once the lighting changed, and there was sometimes debris or other water agitation that interfered with clean views of the propeller blades (Figure 30). Sheet cavitation occurs directly on the face of the blade so it can be difficult to identify when the blade is not fully visible, and even when the blade is fully in frame, the camera angles were such that it was not possible to see if the foam or bubbles were actually in contact with the blades or floating around them (Figure 26). Cloud cavitation happens behind the blade (or in the direction opposite of craft movement), and as there were only cameras mounted on one side of the propeller, the opposite face was never captured. Cloud cavitation is also hard to identify with murky or agitated water, and the exhaust being released from the propeller sometimes hung as a cloud of darker haze around the propeller area and obscured other hazes or foams that might actually be cloud cavitation.

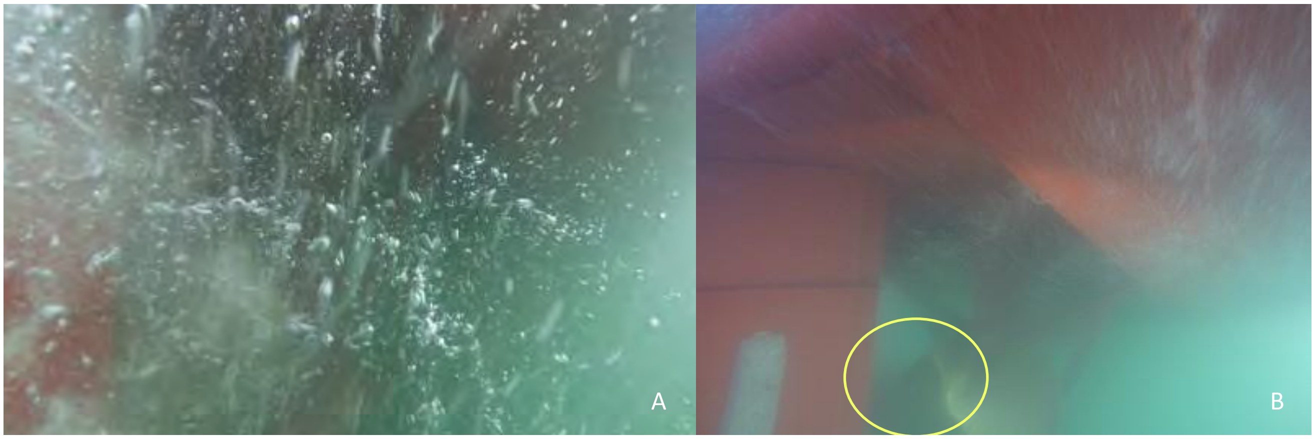


**Figure 30. An example of the view of the propeller being obscured by A) water agitation and B) by exhaust being released (in yellow circle).**

Further to the issue of water agitation is the fact that water is a dynamic environment. It was not always possible to identify which bubbles around the propeller were caused by blade action and which may have been the result of water contact with the hull of the boat, or indeed of water interaction with itself (the trials were run during rising tide so there was water entering the harbour during the trials). These non-propeller caused events did interact with the water movements caused by the propeller, as can be seen in Figure 31. In this example, a random chain of bubbles appeared from below (image A). When the chain reached the point where it was sufficiently impacted by the water motion generated by the propeller blades, it began to twist and waver (image B). The force of the water movement from the blades was strong enough to disrupt the chain formation (image C). Finally, the bubble scattered and were flung out as individual or paired bubbles, with the violence of the motion noticeable in the streaking of their movement in the video capture (image D). In another example, when the vessel was moving faster or encountered waves, there could be a lot of fast-moving bubbles in the field of view (Figure 32).

In section 3.2.2.1 it was noted that it was not possible to directly link changes in the number of observed moments of vortex cavitation to the velocity or acceleration of the vessel at the time, and that the formation of the vortices did not seem to be related to the direction of the vessel in relation to the current winds during the trials. What was noted in the video imagery analysis, however, was that vortex cavitation was frequently seen soon after the rudder of the vessel shifted, especially when it was a large shift (e.g., moving from port to starboard). This would suggest that the changes in the movement of the vessel have a significant part to play in the environment that causes vortex cavitation to occur with the Acadian propeller model; future studies would need to be designed to collect data from times of change in direction as well as during single-direction sea trial runs such as were the focus of this project.

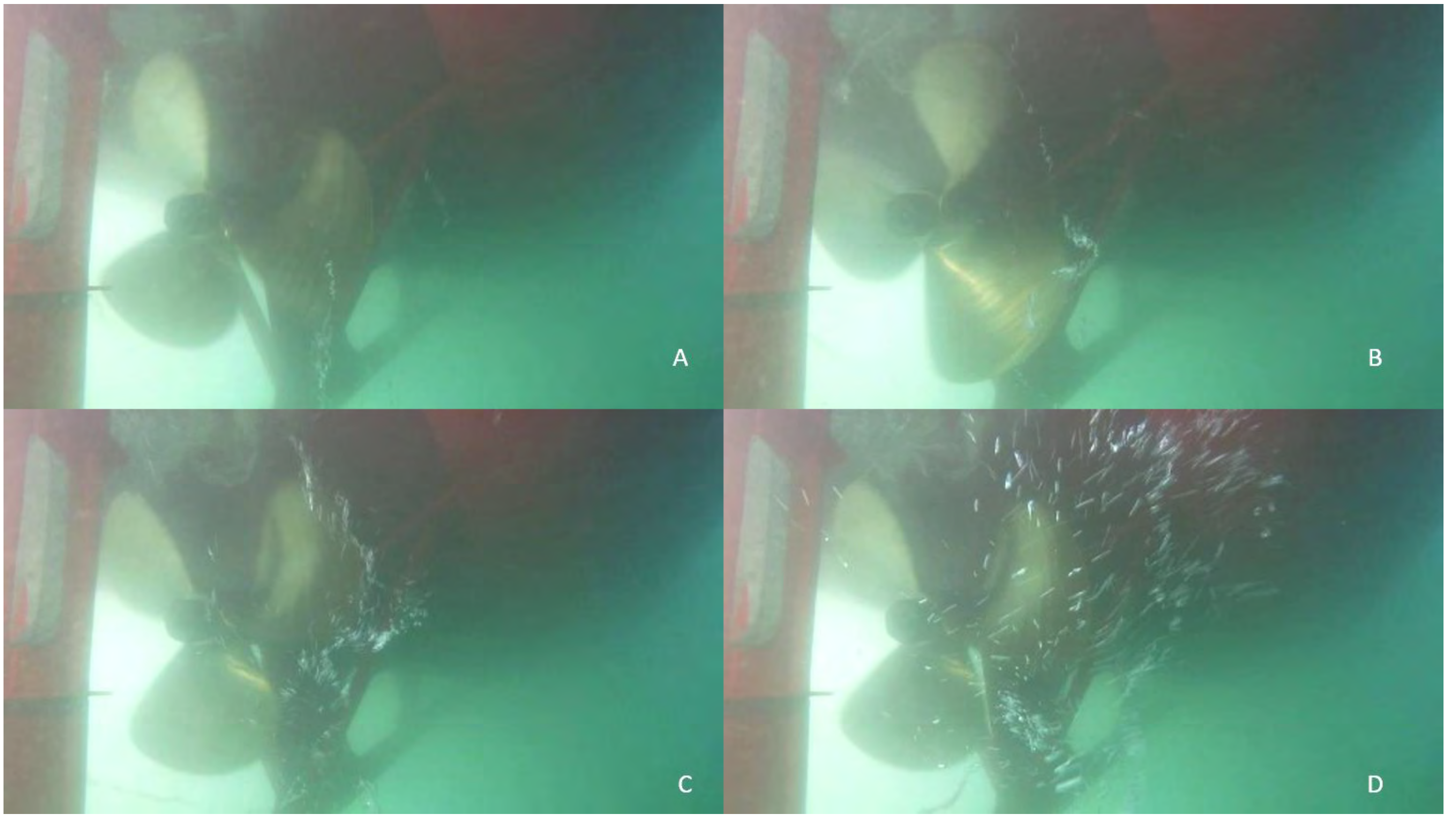


**Figure 31. A random chain of bubbles interacts with the propeller's water dynamic. A. A chain of bubbles enters the propeller area from below. B. The chain starts to twist as it encounters the water movement generated by the propeller blades. C. The chain is disrupted. D. The bubbles are flung violently out of the propeller area.**

**Figure 32. The camera field of view obscured by fast moving bubbles either caused by the speed of the vessel or by the rising tide (or both).**

It was discovered during the review of sea trial imagery and the still images were not captured at a rate that was adequate for the speed at which events were occurring. One image might show the beginning of foam around the outer edge of a blade, and the next would show a fully developed vortex ring floating beside the propeller. Looking at the video frame by frame when there was cavitation activity and saving screen captures allowed a much greater understanding of what was occurring around the propeller blades. The video was filmed at a rate of 30 frames per second – if it had been possible to capture it at a faster rate such as 60 frames per second, then a smooth high-quality slow-motion clip of each cavitation event could be produced for further examination.

Along with camera speed, another issue identified was the focal range – the cameras used were too far from the blades to capture images of fine bubbles developing on the blade surface – the images would only document it once a mass of bubbles became big enough to appear as bluish or whitish foam on or along the blade. Having a camera with a tighter focus on one blade could help in documenting bubble or sheet cavitation.

One tremendous impact on the data collection during the sea trials was the dislodging of the GoPro camera that was collecting video footage. Figure 33 displays how the camera slowly shifted throughout the course of the sea trials, with image A being from the earliest part of the day. Image B shows how the camera started tilting downwards, no longer capturing the top of the blade sweep path; during the review, it was noted that this downwards shift occurred after the rudder was adjusted. Image C, taken during trial 4, is the last clear image of the propeller obtained by this camera; immediately after this image, the camera shifted so that only the rudder strut was visible (Image D). As the sea trials got progressively faster in speed, this means that there is no video of the fastest movements of the propeller during trials 5 and 6. It is to be noted that the GoPro camera taking still images also shifted through the trials, but never completely lost view of the propeller area.

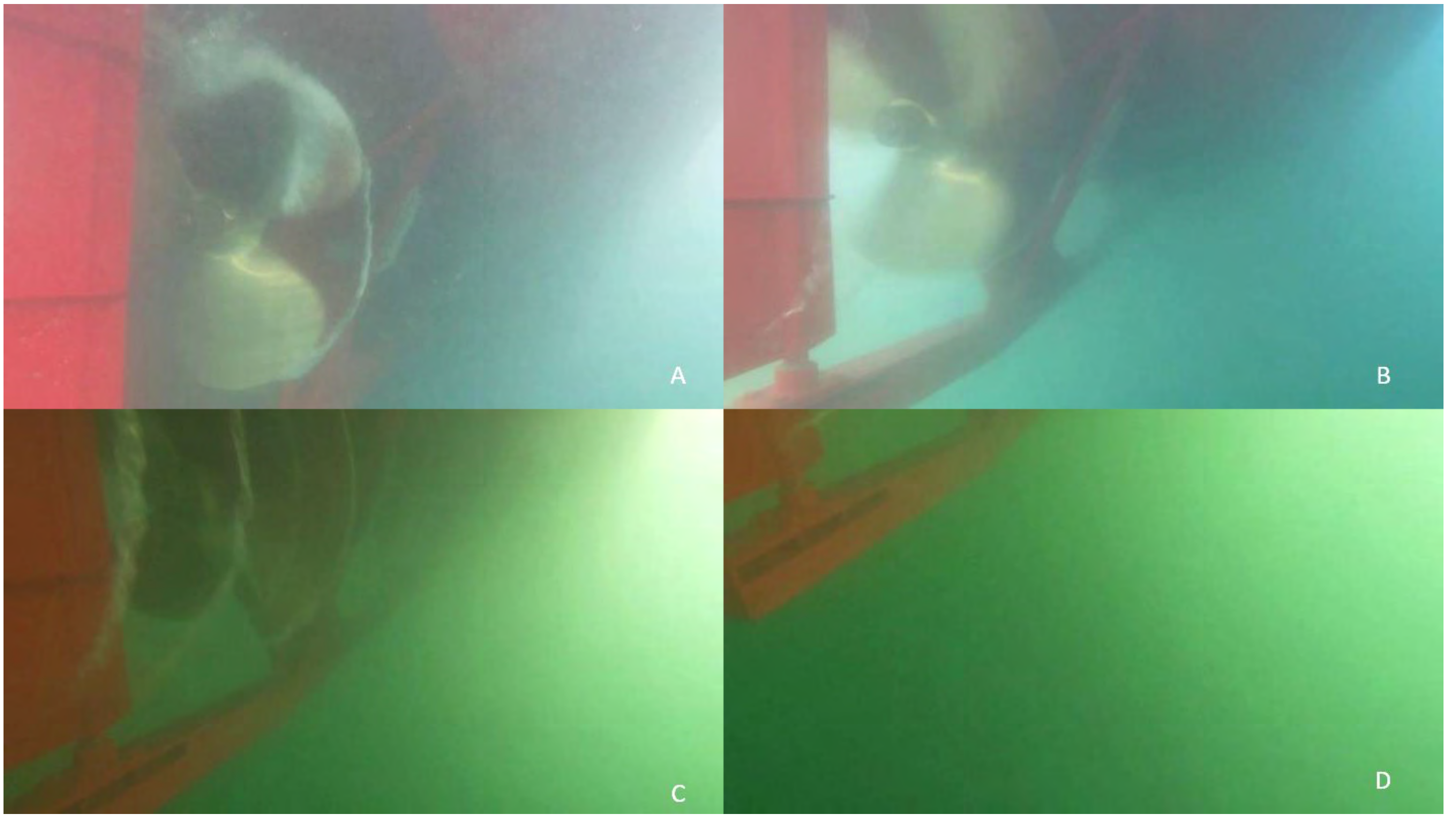


**Figure 33. The slow dislodging of the GoPro camera capturing video footage can be seen in this series of screen captures from various times throughout the course of the sea trials.**

During the review of the sea trial data, it became apparent that the GoPro camera that was recording video had not been synchronized with the GoPro that was collecting still images and the GNSS equipment. The video screen captures had to be matched to still images to get the associated GNSS point to get vessel velocity and acceleration. The visual matching of specific events was complex: the cameras had different angles on the propeller, and so what was visible in one was not the same as in the other imagery, and the different frame rate of capture meant that a phenomenon seen in a screen capture from the video saved at 30 frames per second might not have been present at all in the still imagery taken at 3 frames/2 seconds. It was determined that the timestamp on the video of the launch and first trial was out of sync by approximately 51 seconds, and the second video file than included footage of trials 2 through 6 was out of sync by approximately 1 minute and 32 seconds.

The LIFE participants noted that dive light battery was exhausted when it was inspected after the trials. It is not known when exactly the light exhausted its power supply, but the still images collected at the end of the trials still had enough illumination for the blades to be visible so it may not have occurred until after the trials had been completed. This issue may have had a greater impact if the video camera had still been operational past the midpoint of the trials, as it was deeper in the water and thus needed more illumination.

# 5 Conclusion

NSCC-AGRG produced 3D models of three propeller models using photogrammetric techniques. This work was followed up by sea trials that assessed a propeller's performance characteristics such as cavitation and vibration and examined them in relation to vessel velocity and acceleration. Several important lessons were learned over the course of the project:

1) photographs produced superior 3D models in comparison to laser scans of the propellers;
2) video was the best method to capture the propeller motion and formation of vortices and bubble masses;
3) video viewed in slow motion gives the best opportunity for understanding cavitation events, so a frame rate of 60 frames per second is desirable;
4) all equipment recording data must be synchronized so data can be matched up appropriately for review and analyses;
5) additional camera views, such as from both in front of and behind the propeller and a cross-section view (looking from one side of the propeller area to the other) would allow more of the propeller area to be recorded, allow for different focal lengths to be captured, and allow the possibility of at least one camera continuing to capture imagery even when the view of others has been obscured by water agitation;
6) AGRG experienced the efficacy of having a mounting system to position and secure recording equipment during data collection and is interested in designing a mobile equipment mounting system of their own;
7) a more secure mounting system is required for underwater data collection, as both GoPro cameras shifted and the propeller was not in the center of the field of view at the highest speed trials;
8) the shifting of the cameras occurred in close association with an observed rudder shift, indicating that care must be taken in changing the movement of the vessel in order to minimize impact on the recording equipment; and
9) based on observations, data needs to be collected during changes in vessel direction so perhaps a slalom-style course of continuous s-curves or small shifts in direction should be sailed as well as a straight-line one.

The results of this project will not likely lead to modification of the propeller design or construction process to improved performance. However, future projects building on this could involve sailing a course with more direction changes and testing other vessels of variable hull design (size and shape) as well as integrating an Inertial Measurement Unit to measure the vessels' attitude and vibration at a higher frequency than the 2 Hz measurements using the GNSS.

# 6 References

Cult of Sea. (n.d.) *Cavitation – Propeller Phenomena – Cause, Types & Avoidance.* Cavitation - Propeller Phenomena - Cause, Types, Effects & Avoidance (cultofsea.com)

HydroComp, Inc. (2007). *Blade Area Ratio Defined. A HydroComp Technical Report, Report 135*. http://www.hydrocompinc.com/

# Appendix A: Tables of calculations of Blade Area Ratios

## A1: Method of calculating "Developed" Blade Area Ratio (DAR)

| Procedure | Propeller | | |
|---|---|---|---|
| | **Grand Banks** | **Bluenose** | **Acadian** |
| 1. The generated 3D propeller mesh was imported into Fusion 360. |  |  |  |
| 2. Software tools were used to excise one blade from the rest of the propeller |  |  |  |
| 3. Blade was converted from mesh to body (software object types) | | | |
| 4. Software measures area of object = total surface area of blade (both sides) | | | |
| Surface area of total blade | 1,938 $cm^2$ | 1,890 $cm^2$ | 1,903 $cm^2$ |

| Procedure | Propeller | | |
|---|---|---|---|
| | Grand Banks | Bluenose | Acadian |
| 5. Divide the surface area of blade (#4) by 2 to get surface area of one side. | | | |
| Surface area of one side | 969 $cm^2$ | 945 $cm^2$ | 951.5 $cm^2$ |
| 6. Total blade surface area = surface area one side of blade (#5) X number blades on propeller model | | | |
| Total blade surface area | 2,907 $cm^2$ | 3,780 $cm^2$ | 2,854.5 $cm^2$ |
| 7. Total propeller area for the full propeller was determined by using the radius of the propeller and $A = \pi r^2$ | | | |
| Total propeller area | 5,188.68 $cm^2$ | 5,188.68 $cm^2$ | 5,188.68 $cm^2$ |
| 8. Hub area of the propeller was determined using radius of hub and $A = \pi r^2$ | | | |
| Hub area | 96.77 $cm^2$ | 109.36 $cm^2$ | 91.61 $cm^2$ |
| 9. Blade Arc = Total propeller area (#7) – hub area (#6) | | | |
| Blade Arc | 5,091.91 $cm^2$ | 5.079.32 $cm^2$ | 5,097.07 $cm^2$ |
| 10. "Developed" Blade Area Ratio = Total propeller area (#7)/blade arc (#8) | | | |
| "Developed" Blade Area Ratio | 0.57 | 0.74 | 0.56 |

## A2: Method of calculating "Projected" Blade Area Ratio (PAR)

| Procedure | Propeller | | |
|---|---|---|---|
| | Grand Banks | Bluenose | Acadian |
| 1. Blades created in DAR step 2 used in this calculation also |  |  |  |
| 2. Use the following trigonometry to calculate apparent areas of blades:<br>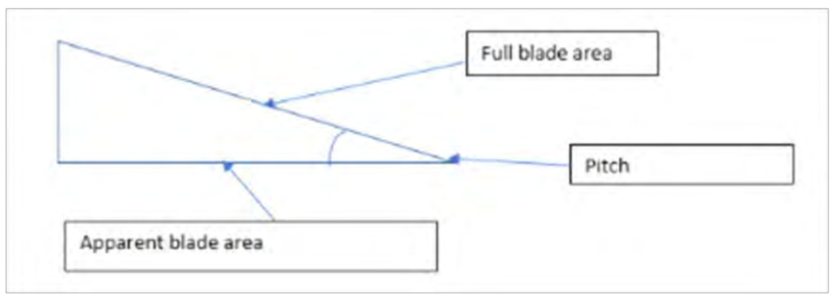 | | | |
| 3. A is the pitch of the blade (provided by manufacturer), c is the surface area of one side as calculated DAR #4, and C is known as the angle between the blade and hub. | | | |

| Procedure | Propeller | | |
|---|---|---|---|
| | **Grand Banks** | **Bluenose** | **Acadian** |
| 4. Drawings showing calculated trig results | 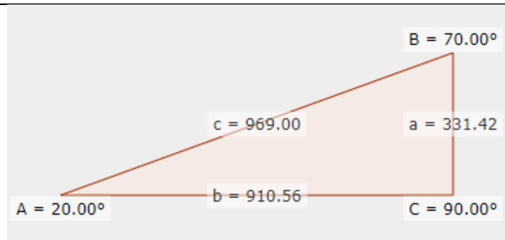  | 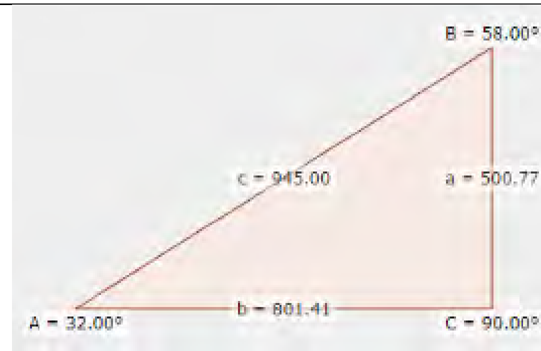  | 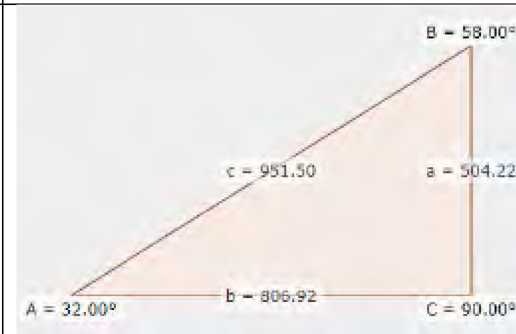  |
| 5. Apparent blade area (b in diagram) | 910.56 $cm^2$ | 801.41 $cm^2$ | 806.92 $cm^2$ |
| 6. Total blade area (apparent blade area (#5) X number of blades) | | | |
| Total blade area | 2,731.69 $cm^2$ | 3,205.64 $cm^2$ | 2,420.76 $cm^2$ |
| 7. "Projected" Area Ratio = total apparent blade area (#6)/blade arc (DAR #9) | | | |
| 8. "Projected" Area Ratio | 0.53 | 0.63 | 0.47 |

## A3: Method of Verifying calculations using HydroComp Conversion formula (2007)

The HydroComp formula offers a way to calculate approximate conversions between the three types of BAR; we are using it as a way to verify our calculations: the calculated PAR and DAR will be used and compared to the results of performing the right side of the formula with the pitch and diameter provided by the manufacturer.

HydroComp Conversion formula

$$\frac{PAR}{DAR} = 1.067 - 0.229\ X\ P/D$$

Where:

PAR = "Projected" Blade Area Ratio　　DAR = "Developed" Blade Area Ratio

P = Blade Pitch　　D = Propeller Diameter

| Calculation | Propeller | | |
|---|---|---|---|
| | **Grand Banks** | **Bluenose** | **Acadian** |
| |  |  |  |
| PAR | 0.53 | 0.63 | 0.47 |
| DAR | 0.57 | 0.74 | 0.56 |
| PAR/DAR | 0.929 | 0.851 | 0.839 |
| HydroComp Conversion | 0.924 | 0.838 | 0.838 |

## Appendix B: Table of vortex cavitation incidents that occurred outside of the sea trials.

| Image | Time (UTC) | Velocity | Acceleration | Comment |
|---|---|---|---|---|
|  | 14:11:28 | Before GNSS equipment started | Before GNSS equipment started | Vortex building – first ring visible to right of blades, with next building in foam at top. Blades slowed down near end of this instance. |
| 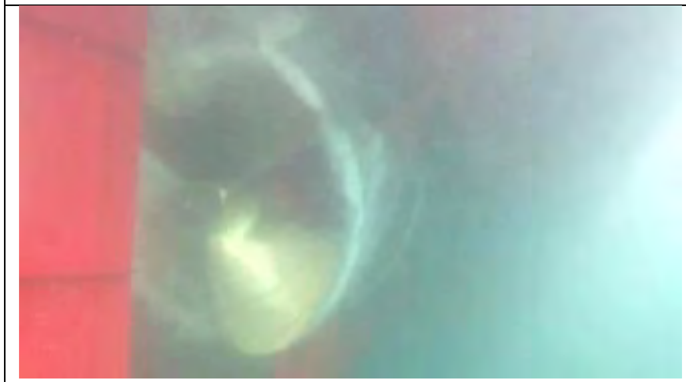 | 14:11:37 | Before GNSS equipment started | Before GNSS equipment started | Immediately after blades restarted from instance above. Taken after vortex more developed, can see multiple rings behind propeller. |
|  | 14:12:36 | Before GNSS equipment started | Before GNSS equipment started | Cavitation appeared to stop part way through this stretch, and then vortex reformed. |

| Image | Time (UTC) | Velocity | Acceleration | Comment |
|---|---|---|---|---|
| 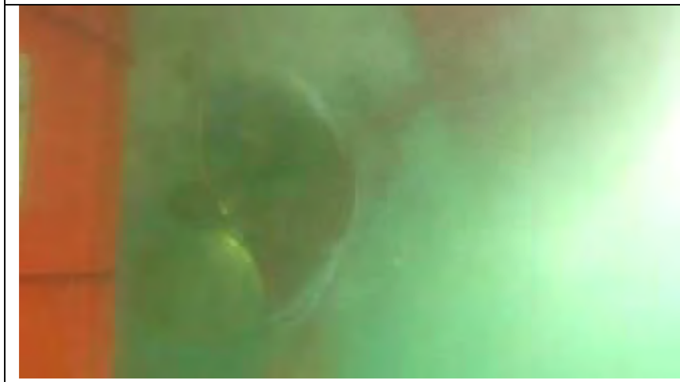 | 14:12:51 | Before GNSS equipment started | Before GNSS equipment started | Lots of fine foam behind propeller during this instance. |
|  | 14:12:59 | Before GNSS equipment started | Before GNSS equipment started | A rapid change in propeller direction quickly started this vortex incident, which is characterized by foamy, diffuse rings. |
| 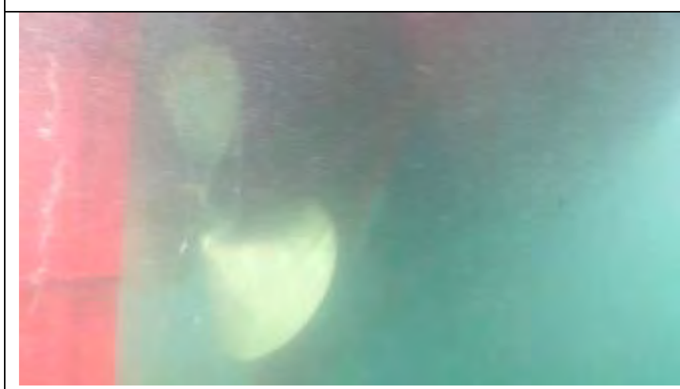 | 14:13:13 | Before GNSS equipment started | Before GNSS equipment started | Four faint vortex rings visible from blades towards rudder. |

| Image | Time (UTC) | Velocity | Acceleration | Comment |
|---|---|---|---|---|
|  | 14:13:30 | Before GNSS equipment started | Before GNSS equipment started | A vortex ring appears to be interacting with a burst of bubbles that had suddenly appeared moving upwards from offscreen. |
| 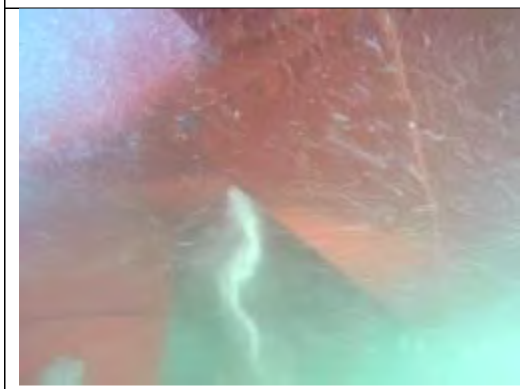 | 14:28:54 | After GNSS equipment stopped | After GNSS equipment stopped | Sudden cohesive white line (vortex? See twisting in strands at bottom) hanging off bottom of boat down towards blade area, brighter than when it first appeared in previous image in sequence. |